ELSEVIER

Journal of Organometallic Chemistry 576 (1999) 254–278

Journal of Organometallic Chemistry

Review

Mechanistic and kinetic studies of palladium catalytic systems☆

Christian Amatore *, Anny Jutand [1]

Ecole Normale Supérieure, Département de Chimie, CNRS URA 1679, 24 Rue Lhomond, F-75231 Paris Cedex 5, France

Received 1 August 1998

Abstract

It is established that new reactive anionic palladium(0) complexes species are formed in which palladium(0) is ligated by either chloride ions: $Pd(0)(PPh_3)_2Cl^-$ (when generated by reduction of $PdCl_2(PPh_3)_2$) or by acetate ions: $Pd(0)(PPh_3)_2(OAc)^-$ (when generated in situ in mixtures of $Pd(OAc)_2$ and PPh_3). The reactivity of such anionic palladium(0) complexes in oxidative addition to aryl iodides strongly depends on the anion born by the palladium(0). The structure of the arylpalladium(II) complexes formed in the oxidative addition also depends on the anion. Indeed, intermediate anionic pentacoordinated arylpalladium(II) complexes are formed: $ArPdI(Cl)(PPh_3)_2^-$ and $ArPdI(OAc)(PPh_3)_2^-$, respectively, whose stability depends on the chloride or acetate anion brought by the palladium(0). $ArPdI(Cl)(PPh_3)_2^-$ is rather stable and affords *trans* $ArPdI(PPh_3)_2$ at long times via a neutral pentacoordinated solvated species $ArPdI(S)(PPh_3)_2$ involved in an equilibrium with the chloride ion. $ArPdI(OAc)(PPh_3)_2^-$ is quite unstable and rapidly affords the stable *trans* $ArPd(OAc)(PPh_3)_2$ complex. Consequently, the mechanism of the $PdCl_2(PPh_3)_2$-catalyzed cross-coupling of aryl halides and nucleophiles has been revisited. The nucleophilic attack does not proceed on the *trans* $ArPdI(PPh_3)_2$ complexes as usually postulated but on the intermediate neutral pentacoordinated species $ArPdI(S)(PPh_3)_2$ to afford a pentacoordinated anionic complex $ArPdI(Nu)(PPh_3)_2^-$ in which the aryl group and the nucleophile are adjacent, a favorable position for the reductive elimination which provides the coupling product Ar–Nu. The mechanism of the Heck reactions catalyzed by mixtures of $Pd(OAc)_2$ and PPh_3 has also been revisited. The nucleophilic attack of the olefin proceeds on $ArPd(OAc)(PPh_3)_2$ and not on the expected *trans* $ArPdI(PPh_3)_2$ complex which is never formed when the oxidative addition is performed from $Pd(0)(PPh_3)_2(0Ac)^-$. This work emphasizes the crucial role played by the anions born by the precursors of palladium(0) complexes and rationalize empirical findings dispersed in literature concerning the specificity of palladium catalytic systems.

Keywords: Palladium catalyst; Oxidative addition; Cross-coupling; Mechanism; Heck reaction

1. Introduction

Among the catalysts of organic reactions palladium is the most versatile one since it catalyzes the formation of C–C, C–H, C–N, C–O, C–P, C–S and C–CO–C bonds from reactions of aryl halides/triflates, vinyl halides/triflates, allylic derivatives with *nucleophiles* [1] (cross-coupling reactions [1a,b,e,h,j,m], Stille reactions [1d,e,h,m], Suzuki reactions [1h,i,m], Heck reactions [1b,c,e–h,j,m], Tsuji–Trost reactions [1c,f,h,j–m]. In the presence of an electron source, the reactivity is reversed and reactions with *electrophiles* allow the formation of C–C, C–H and $C-CO_2$ bonds [2].

The efficiency of palladium originates from its ability, when it is zerovalent, to activate C–X bonds (X = I [3], Br [3b], Cl [3b], O [4]) by an oxidative addition which provides an organopalladium(II) complex prone to react with nucleophiles [5,6]. The nucleophilic reac-

☆ Dedicated to Professor Richard F. Heck and to Professor Jiro Tsuji.

* Corresponding author. Tel. +33-1-44323388; fax: +33-1-44323325.

[1] Also corresponding author.

0022-328X/99/$ - see front matter
PII: S0022-328X(98)01063-8

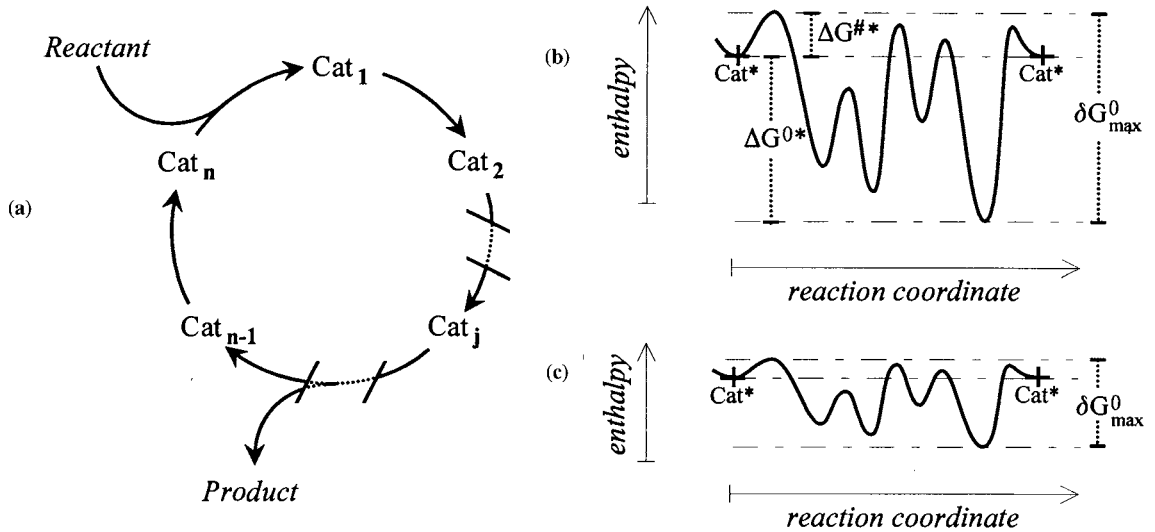

Scheme 1.

tion provides a new organopalladium(II) complex which affords the final compound after one or several steps [6]. A large variety of palladium(0) complexes are used as catalysts, either isolated complexes such as $Pd(0)L_4$ (L = phosphines) or complexes generated in situ from mixtures of $Pd(0)(dba)_2$ and phosphines. Palladium(II) complexes, PdX_2L_2 (X = Cl, Br, I) are also used as precursors of palladium(0) complexes, in the presence of a reducer, very often the nucleophile itself. When the later is not able to reduce the palladium(II) complex, an external reducer is required such as hydrides, Grignard, organolithium, zinc or aluminum reagents. Another source of palladium(0) complexes consists in mixtures of divalent $Pd(OAc)_2$ and phosphine ligands. Through considerable empirical testing of different catalytic systems, $Pd(0)L_4$ complexes have been proven to be more or less able to catalyze reactions with almost all kinds of nucleophiles whereas the three others sources of palladium(0) complexes appear to be more specific of a given reaction. Mixtures of $Pd(0)(dba)_2$ and phosphines are used frequently in allylic substitutions (Tsuji–Trost reactions). Mixtures of $Pd(OAc)_2$ and phosphine ligands are efficient in Heck reactions and PdX_2L_2 in cross-coupling and Stille reactions. This classification should not be taken too strictly since it requires some nuances and restrictions. Indeed, some Heck reactions are catalyzed by $Pd(0)L_4$ complexes, however in the presence of acetates as a base [1f]. $Pd(0)(BINAP)_2$ catalyzes asymmetric Heck reactions provided acetate ions were present [7].

The efficiency of the palladium catalyst is expected, of course, to strongly depend on the ligand of the palladium atom. However, for a given ligand, it is surprising that the overall reactivity also depends on the precursor of the palladium(0) complex since there is a general agreement on the fact that the low ligated, 14-electron $Pd(0)L_2$ complex is always the active species which initiates the catalytic cycle via its oxidative addition [1].

In order to understand why different sources of palladium(0) are so specific, we investigated the structure and the reactivity of the different resulting palladium(0) complexes in oxidative additions. Moreover, since the oxidative addition might not be the rate determining step of the catalytic cycle, the structure of the organopalladium(II) complexes resulting from the oxidative addition was also investigated as well as their reactivity in the further step of a real catalytic cycle, i.e. their reaction with nucleophiles. All these investigations have been made in the context of a catalytic cycle sequence, i.e. starting from the real precursors of the palladium(0) complexes. The alternative and more spread approach consists in investigating mechanisms at the stoichiometric level on separated and independent steps, i.e. not in the context of the overall catalytic reaction. However, despite their intrinsic independent value, such studies very often give rise to erroneous results since they are often performed with isolated (and thus stable) complexes that might not be the real reactive species involved in the considered step when this step belongs to a catalytic sequence instead of a stoichiometric reaction. By this method, intermediate complexes may be overlooked although they may play a crucial role in the catalytic reaction. Moreover, investigation of mechanisms by studying one step independently from the previous one, i.e. not in the chemical context of the previous one, very often results in the by-pass of the role of presumed innocent species such as anions or cations which are present in the catalytic sequence and not in the isolated step model and which may even induce changes of the rate determining step.

In any catalytic cycle, the total amount $[Cat]_{tot}$ of catalyst is present under several reactive forms, Cat_1, Cat_2,..., Cat_n, which are distributed all along the catalytic sequence (see Scheme 1a), and the available concentration of each of these forms of the catalyst is regulated by steady state considerations. At most, the relative concentration of each of the catalytic forms is given by the thermodynamic Boltzman distribution, so that one has:

$$[Cat_j] \leq [Cat]_{tot} \times \exp(-\Delta G_j^0/RT)/[\Sigma_{1,n} \exp(-\Delta G_h^0/RT)]$$

where ΔG_j^0 is the free enthalpy difference between the catalyst form Cat_j and the most stable one taken as a reference.

On the other hand, whenever the catalytic cycle is very efficient, the rate of each of its chemical steps is equal because of the steady state requirement. Therefore, the rate of the catalytic cycle can be evaluated by considering, for example the step which involves the catalytic species of the highest energy. Let Cat* be this species, and k^*, the rate constant of its chemical reaction (note that the reaction involves a bimolecular step with a reactant Z, $k^* = k_0^* \times [Z]$). Thus, owing to the above equation, the maximum rate of the cycle is:

$$v_{max} \leq k^* \times [Cat]_{tot} \times \exp(-\Delta G^{0*}/RT)/[\Sigma_{1,n} \exp(-\Delta G_h^0/RT)]$$

Considering for example an Eyring formulation for k^* (or for k_0^*), one obtains:

$$v_{max} \leq (kT/h) \times [Cat]_{tot} \times \exp[-(\Delta G^{\#*} + \Delta G^{0*})/RT] /[\Sigma_{1,n} \exp(-\Delta G_h^0/RT)]$$

or for a bimolecular step with a collision frequency $\mathscr{Z}$:

$$v_{max} \leq \mathscr{Z} \times [Cat]_{tot}[Z] \times \exp[-(\Delta G^{\#*} + \Delta G^{0*})/RT] /[\Sigma_{1,n} \exp(-\Delta G_h^0/RT)]$$

where $\Delta G^{\#*}$ is the enthalpic barrier relative to the reaction of species Cat*.

One can note $\delta G_{max}^0 = (\Delta G^{\#*} + \Delta G^{0*})$. δG_{max}^0 is by definition the energetic span of the cycle, i.e. the enthalpy difference between the point of highest energy and that of lowest energy along the energetic path of the catalytic sequence along one cycle of the reaction (see Scheme 1b). Therefore the maximum rate of the cycle is given by:

$$v_{max} \leq (kT/h) \times [Cat]_{tot} \times \exp(-\delta G_{max}^0/RT)/[\Sigma_{1,n} \exp(-\Delta G_h^0/RT)]$$

for a first order reaction of Cat* or by:

$$v_{max} \leq \mathscr{Z} \times [Cat]_{tot}[Z] \times \exp(-\delta G_{max}^0/RT)/[\Sigma_{1,n} \exp(-\Delta G_h^0/RT)]$$

for a second order reaction.

Whatever is the case, it is thus obvious that v_{max} is the largest possible when δG_{max}^0 is the smallest possible. In other words, the smallest δG_{max}^0 is, the fastest the catalysis.

We wished to recall here this elementary result of catalysis to show that the most common tentatives of improving a catalytic cycle by improving the rate of its slowest steps (i.e. precisely that one which implies the species of lesser availability, that is Cat* here) has no chance of success if the catalytic sequence is preserved otherwise. Indeed, based on Hammond postulate, one generally try to make the species more reactive by increasing its energy, so that $\Delta G^{\#*}$ decreases. Obviously, this strategy is efficient under stoichiometric conditions where the catalytic cycle has to rotate only once (or only a few times) to complete the reaction. Yet under true catalytic conditions the result is opposite because the gain in lowering $\Delta G^{\#*}$ is more than lost by the loss due to the increase in ΔG^{0*}, so that the net effect is that δG_{max}^0 increases and v_{max} decreases. This can be easily verified by considering that the gain in $\Delta G^{\#*}$ is at most $-\beta \times \Delta(\Delta G^{0*})$, where β is the Brönstedt coefficient of the step considered and $\Delta(\Delta G^{0*})$ is the positive variation of $\Delta(\Delta G^{0*})$ due to the fact that the stability of species Cat* has been decreased to make it more reactive. Therefore the net effect on δG_{max}^0 is $(1-\beta) \times \Delta(\Delta G^{0*})$, and since $\beta \leq 1$, the net effect is that that $\Delta(\delta G_{max}^0)$ is positive or at best negligible when $\beta \approx 1$.

In other words, even if the cycle proves better under stoichiometric conditions or nearly stoichiometric ones (viz. only a few rotations are required), it will be slower under catalytic ones. This surprizing result is apparently contradictory with common considerations. However, and albeit not usually cast in these terms, this result is well known in catalysis. Indeed, consider for example the poisoning of a catalytic sequence. Poisoning consists in fact into a considerable stabilization of one of the catalyst reactive forms generally by a down-hill but reversible complexation, etc. In other words, this amounts to considerably increase δG_{max}^0 and therefore decrease considerably v_{max}. Fundamentally, what is happening is that the poison is killing the catalytic sequence because it stores almost all the catalyst under a too much stable form. Considering this example, one should easily understand that destabilizing the most unstable forms of the catalyst amounts to do the same, i.e. to poison the cycle, since what matters is only enthalpy differences and variations and not true enthalpy values.

A correlate to this conclusion is obviously that one makes the catalytic sequence the fastest possible by

making the energy span δG^0_{max} the smallest possible, even if that has the opposite effect for stoichiometric conditions. In other, to increase the rate of a catalytic conversion, one needs to stabilize the catalytic forms of highest energy and destabilize those of the lowest energy, so that the net effect is to lessen δG^0_{max} (see Scheme 1c). In this review, we will show several examples of such situations, in which the positive effect of added ions is readily explained by such considerations. Albeit these ions (i.e. halides, acetate, etc.) do not participate *chemically* in the real chemical sense in the catalytic efficiency, they contribute efficiently to the catalytic sequence by a considerable shrinking of the energy span δG^0_{max} of the cycle.

We wish to discuss in this review some mechanistic investigations on palladium-catalyzed reactions taking into account the precursor of the palladium(0). They result in the discovery of new organometallic species and consequently new catalytic cycles are proposed which rationalize some empirical results observed in literature.

2. Methods for the investigation of the mechanism of transition metal-catalyzed reactions

Transition metal-catalyzed reactions proceed by catalytic cycles involving metal complexes in different oxidation states. Most metal complexes are either oxidized or reduced or both. Consequently they are easily detected and characterized by means of electrochemical techniques (voltammetry, amperometry, chronoamperometry…etc) and their reactivity monitored by the same techniques taking advantage of the fact that reduction/oxidation currents are proportional to the species concentration.

Two approaches are available:

- *Steady state voltammetry* is used as an analytic technique to characterize a metal complex already present in solution. It is characterized by its reduction/oxidation potential and its concentration determined by the value of its reduction/oxidation current. Its reactivity with a substrate can be investigated by monitoring the evolution of its reduction/oxidation current as a function of time, by means of a rotating disk electrode which provides sigmoid shaped waves whose plateau currents are proportional to the species concentration. Moreover, if a new electroactive metal complex is formed during the course of the reaction, it may also be detected and characterized by its reduction/oxidation peak and the yield of the reaction determined by the value if its reduction/oxidation current. Thus, it is possible to characterize the reagents and the products of a chemical step as well as its kinetics. This steady state technique is then similar in principle to spectroscopic methods and affords kinetic data for chemical reactions with half-reaction times $t_{1/2}$ higher than a few tens of seconds.

  Transient voltammetry evidences for the existence of an equilibrium between different complexes by the relative variation of the reduction/oxidation peak current of the different species when the scan rate is varied. Scan rate fixes the time scale of the experiment. The reduction/oxidation of one species at the electrode surface causes a continuous shift of the equilibrium in the diffusion layer and the concentration of the species, measured by its reduction/oxidation current, does not reflect its true concentration but a dynamic concentration (CE mechanism [8]). For shorter and shorter times, the equilibrium is less and less easily shifted and for very short times (high scan rates), a dynamic equilibrium is frozen while it is perfectly labile at long times (low scan rates). This allows the determination of the equilibrium concentrations of the different complexes and then the equilibrium constant. The thermodynamics and kinetics of the equilibrium can thus be characterized by transient voltammetry or by potential step chronoamperometry performed during a time θ on the reduction/oxidation waves of the different species. In this context, electrochemical methods are more akin to NMR spectroscopy since the progressive freezing of an equilibrium upon increasing the scan rate (voltammetry) or shortening the pulse duration θ (chronoamperometry) is analogous to coalescence in NMR spectroscopy.

  In cases of equilibrated reactions, the species observed as the major one in solution is not necessary the real reactive one because the later may be involved in an endergonic equilibrium. As for classical techniques able to monitor reactions, the effective reactive species will be identified only through a detailed investigation of the kinetics.
- *Cyclic voltammetry* may also be used to generate, by successive electron transfers and chemical steps, stable or short-lived organometallic species, by reduction/oxidation of metal complexes. Knowledge of the absolute number of electron(s) involved in any electrochemical process allows the determination of the oxidation state of the cascade of complexes which may then be electrogenerated from a given stable complex [9]. Again the kinetics of the electrogenerated species with a choice substrate can be monitored by increasing the scan rate of the cyclic voltammetry (or diminishing the duration of a potential step in chronoamperometry), i.e. by decreasing the time scale for the chemical reaction. Evolution of the voltammogram as a function of the scan rate (or time) affords kinetic data for chemical reactions with half-reaction times $t_{1/2}$ from 0.1 s to 10 ns. Transient species can thus be generated or detected and their reactivity characterized.

Table 1
Comparative reactivity of palladium(0) in the oxidative addition with phenyl iodide as a function of the precursor[a]

No.	Precursor of Pd(0) (2 mmol dm^{-3})	Major species	Reactive species (S = solvent)	k_{app} ($M^{-1}s^{-1}$) 20°C in THF (in DMF)	k_{app} ($M^{-1}s^{-1}$) 25°C in DMF
1	$Pd(0)L_4$	$Pd(0)L_3$	$SPd(0)L_2$	16 (16)	25
2	$PdBr_2L_2+2e$	$Pd(0)L_2Br^-$	$Pd(0)L_2Br^-$	400	
3	$PdCl_2L_2+2e$	$Pd(0)L_2Cl^-$	$Pd(0)L_2Cl^-$	530	
4	$PdCl_2L_2+2e+50Li^+$	Pd(0)L$_2$Cl,Li	Pd(0)L$_2$Cl,Li	1320	
5	$PdCl_2L_2+2e+1Zn^{2+}$	Pd(0)L$_2$Cl,ZnCl	Pd(0)L$_2$Cl,ZnCl	1480	
6	$Pd(0)(dba)_2+2L$	Pd(0)(dba)L$_2$	$SPd(0)L_2$	2.7 (1.9)	
7	$Pd(0)(dba)_2+4L$	Pd(0)(dba)L$_2$	$SPd(0)L_2$	2 (1.3)	
8	$Pd(0)L_4+1AcO^-$	$Pd(0)L_3(OAc)^-$	$Pd(0)L_2(OAc)^-$		21
9	$Pd(OAc)_2+5L$	$Pd(0)L_3(OAc)^-,H^+$	$Pd(0)L_2(OAc)^-,H^+$		41
10	$Pd(OAc)_2+5L+3NEt_3$	$Pd(0)L_3(OAc)^-$	$Pd(0)L_2(OAc)^-$		22
11	$Pd(OAc)_2+3L$	$Pd(0)L_2(OAc)^-,H^+$	$Pd(0)L_2(OAc)^-,H^+$		140
12	$Pd(OAc)_2+3L+3NEt_3$	$Pd(0)L_2(OAc)^-$	$Pd(0)L_2(OAc)^-$		65

[a] "$Pd(0)L_nL'_n$" + $PhI \xrightarrow{k_{app}}$ "$PhPdXL_2$" + $(n-2)L+n'L'$ ($L = PPh_3$).

However, whereas electrochemical techniques allow a fine investigation of the mechanistic features (kinetics and thermodynamics), they cannot afford structural information. Indeed from a reduction/oxidation peak, it is not possible to determine with certainty the structure of a complex unless by comparison to authentic samples. When authentic samples are not available, the structural information shall be provided by combining electrochemical results with other techniques such as ^1H and ^{31}P spectroscopy. Indeed, NMR spectroscopy provides detailed structural information but does not allow a fine investigation of fast kinetics. Thus complementary use of NMR spectroscopy and electrochemical techniques proves essential for the investigation of mechanisms. Similarly, other spectroscopic methods can be combined to provide together with the electrochemical data a detailed kinetic and structural view of a complicated reactive system.

The efficiency of this dual approach for mechanistic studies will be illustrated in the following by the investigation of several elemental steps such as oxidative addition, ligand exchange, insertion, reductive elimination, a series of studies which have been determinant for the elaboration of non-classical but more realistic catalytic cycles.

3. Mechanism of the oxidative addition of aryl halides with palladium(0) complexes as a function of their precursors

In1976, $Pd(0)(PPh_3)_4$ was the first complex tested in cross-coupling reactions of aryl halides with Grignard and organolithium reagents by Fauvarque et al. [5a]. At that time, it was known that the 18-electron complex dissociates in solution to form a stable 16-electron $Pd(0)(PPh_3)_3$ (Eq. (1), S = solvent) [10]. Existence of the 14-electron $Pd(0)(PPh_3)_2$ (Eq. (2)) has been established later on the basis of kinetic studies [11a] which led to the conclusion that the low ligated 14-electron $Pd(0)(PPh_3)_2$ is the actual reactive species in oxidative addition with aryl iodides (Eq. (3)).

$$Pd(0)(PPh_3)_4 \leftrightarrows SPd(0)(PPh_3)_3 + PPh_3 \quad K_1/[PPh_3] \gg 1 \tag{1}$$

$$SPd(0)(PPh_3)_3 \leftrightarrows SPd(0)(PPh_3)_2 + PPh_3 \quad K_2/[PPh_3] \ll 1 \tag{2}$$

$$ArX + SPd(0)(PPh_3)_2 \rightarrow ArPdX(PPh_3)_2 + S \quad k \tag{3}$$

However $Pd(0)(PPh_3)_3$ is the major species in solution. Despite the high reactivity of $Pd(0)(PPh_3)_2$ in the oxidative addition step (3), the overall reaction (4) is slow (Table 1) because the concentration of $Pd(0)(PPh_3)_2$ is maintained at very low levels because of the extremely up-hill nature of the equilibrium (2).

$$ArX + Pd(0)(PPh_3)_4 \rightarrow ArPdX(PPh_3)_2 + 2PPh_3 \quad k_{app} \tag{4}$$

The rate of the overall oxidative addition (Eq. (4)) thus decreases when the concentration of the phosphine increases ($k_{app} = kK_2/[PPh_3]$ [11]), a feature which was crucial in unraveling the role of $Pd(PPh_3)_2$.

Therefore, it is of considerable interest to by-pass equilibrium (2) in order to generate $Pd(0)L_2$ complexes quantitatively in the absence of extra phosphine. This was achieved for the first time in 1976, by using $PdCl_2(PPh_3)_2$ [5a] or $PhPdI(PPh_3)_2$ [12] as a tentative source of $Pd(0)(PPh_3)_2$ when they are reduced by a Grignard reagent. However, despite the efficiency of this strategy at the preparative scale, the fact that the reaction still proceeded through $Pd(0)(PPh_3)_2$ under these conditions remained to establish.

3.1. PdX_2L_2 ($X = Cl$, Br, I) as precursor of $Pd(0)L_2$ ($L = PPh_3$)

$PdX_2(PPh_3)_2$ (X = Cl, Br, I) complexes are reduced in THF in a single reduction peak R_1 (Fig. 1a) [13]. Determination of the absolute number of electron(s) involved in this reduction peak proves it to be a two-electron transfer [9]. Thus, electrochemical reduction of $PdX_2(PPh_3)_2$ (X = Cl, Br, I) affords palladium(0). The later is characterized by its oxidation peak O_1, detected on the reverse scan (Fig. 1a). Double step chronoamperometry performed on the reduction peak and then on the oxidation peak shows that the reduction of the palladium(II) complex to the palladium(0) complex is quantitative. When the reduction of $PdX_2(PPh_3)_2$ (X = Cl, Br, I) is performed in the presence of phenyl iodide, the oxidation peak O_1 of the palladium(0) is no more detected on the reverse scan (Fig. 1b), showing that the oxidative addition of phenyl iodide with the electrogenerated palladium(0) complex is rapid and takes place during the few second duration of the scan [13b]. When the scan rate is increased, i.e. when the time scale for the oxidative addition decreases, the oxidation peak of the palladium(0) is progressively restored. Plotting the variation of the oxidation peak current relative to the initial one *versus* the logarithm of the scan rate affords the kinetics of the oxidative addition (Fig. 2a) and allows the determination of the scan rate $v_{1/2}$ corresponding to the half-reaction time $t_{1/2}$ (viz. $v_{1/2} \propto 1/t_{1/2}$) and thus the rate constant of the oxidative addition (Table 1, entries 2 and 3). As an example, $t_{1/2} = 80$ ms when the palladium(0) is generated by reduction of $PdCl_2(PPh_3)_2$ (2 mmol dm^{-3}) in the presence of PhI (2 mmol dm^{-3}) [13b]. This result demonstrates that transient, short-lived and thus very reactive species can be generated by electrochemical reduction and kinetic data on their reactivity are available (which is impossible with classical analytical techniques, UV, NMR). Under these conditions, the oxidative addition performed from the palladium(0) complex generated by reduction of $PdCl_2(PPh_3)_2$ is more than 30 times faster than that performed from $Pd(0)(PPh_3)_4$ (Table 1) evidencing the inhibiting role of extra PPh_3 due to equilibrium (2) when one starts from $Pd(0)(PPh_3)_4$.

The bielectronic reduction of $PdCl_2(PPh_3)_2$ was supposed to produce the low ligated complex $Pd(0)(PPh_3)_2$. However the ^{31}P-NMR spectrum of this complex, synthesized after an exhaustive electrolysis with consumption of 2 Faradays per mol of $PdCl_2(PPh_3)_2$, exhibits three signals [13b]. The relative magnitude of these three signals depends on the palladium concentration as well as on the chloride concentration (added as *n*-Bu_4NCl prior the electrolysis) suggesting that at least three different palladium(0) complexes are generated by reduction of $PdCl_2(PPh_3)_2$. All the complexes undergo oxidative addition with PhI. The rate of the oxidative

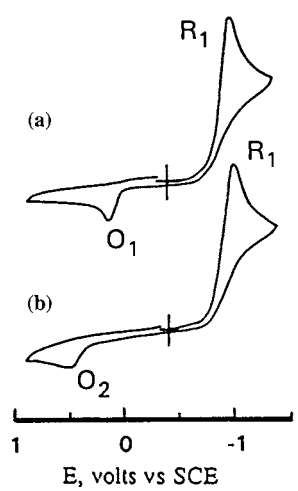

Fig. 1. Cyclic voltammetry of $PdCl_2(PPh_3)_2$, 2 mmol dm^{-3} in THF (containing *n*-Bu_4NBF_4, 0.3 mol dm^{-3}) at a steady gold disk electrode (i.d. 0.5 mm) with a scan rate of 0.2 V s^{-1}. 20°C. (a) $PdCl_2(PPh_3)_2$ alone; (b) in the presence of PhI, ten equivalents.

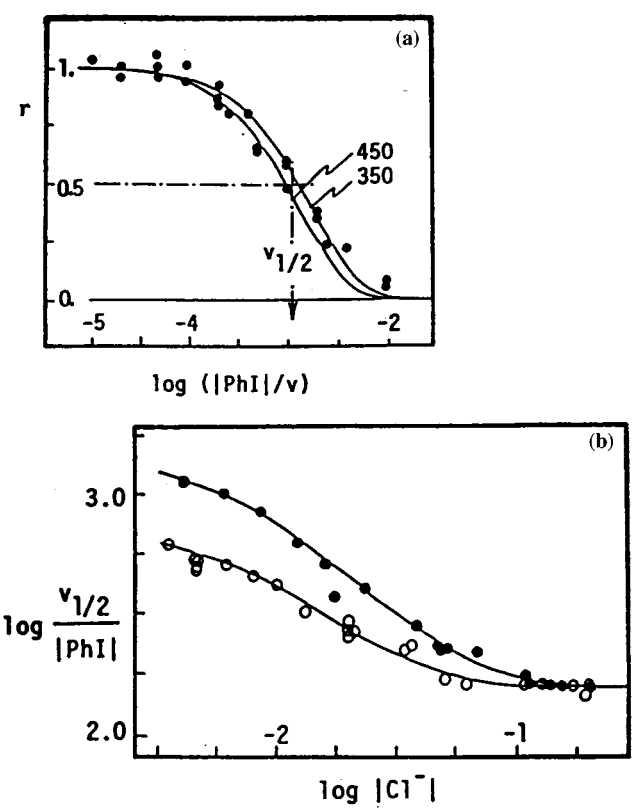

Fig. 2. (a) Cyclic voltammetry of $PdBr_2(PPh_3)_2$, 2 mmol dm^{-3} in THF (containing *n*-Bu_4NBF_4, 0.3 mol dm^{-3}) at steady gold disk electrodes (i.d. 0.5 or 0.125 mm) in the presence of PhI (1–10 equivalents) at different scan rates v ($0.2 < v < 1000$ V s^{-1}). Variation of $r = i_{o_x}(Pd°)/i_{o_x}(Pd°)_0$ *versus* log[PhI]/v. $k = 400$ $M^{-1}s^{-1}$. (b) Oxidative addition of PhI with the palladium(0) generated by reduction of $PdCl_2(PPh_3)_2$. Variation of $\log(v_{1/2}/[PhI])$ *versus* the concentration of Cl^- (introduced as *n*-Bu_4NCl) for $[PdCl_2(PPh_3)_2] = (○)$ 1 and (●) 2 mmol dm^{-3}. Solid lines are simulated curves according to Scheme 2 with $K_{BC} = 70$ M^{-1}, $k_A K_{BA} = 9 \times 10^5$ $M^{-1}s^{-1}$ and $k_C = 72$ $M^{-1}s^{-1}$. 20°C.

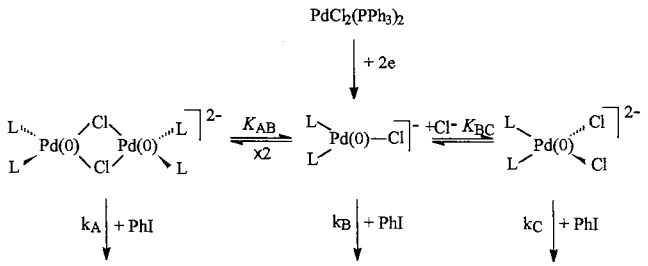

Scheme 2.

addition is slowed down upon decreasing the palladium concentration and increasing chloride ions concentration (Fig. 2b). Therefore, the palladium(0) complex generated by reduction of $PdCl_2(PPh_3)_2$ is ligated by chloride ions to form three anionic species, including one dimer and involved in fast equilibria (Scheme 2).

Resolution of the pertinent kinetic equations affords theoretical curves that fit the experimental voltammetric data (Fig. 2b) [13b]. The dimer is the most reactive species. Yet under usual conditions, its concentration is too low to account significantly in catalytic cycles. Reduction of $PdBr_2(PPh_3)_2$ affords only two mononuclear species (Scheme 3) with $Pd(0)(PPh_3)_2Br^-$ the most reactive one [14].

For a given concentration of halide, the palladium(0) complexes ligated by chloride ions are more reactive than those ligated by bromide ions (Table 1) [13b].

Furthermore, it should be stressed that the halide ligation/deligation reactions in Schemes 2 and 3 are considerably faster than oxidative addition to PhI. Thus, the complex $Pd(0)(PPh_3)_2$ cannot exist in solution as soon as it is generated in the presence of halide ions (borne by the precursor or released during the catalytic cycle). Anionic palladium(0) species are formed by coordination of the palladium(0) center by halides. These results are in agreement with a paper reported by Negishi et al. who proposed for the first time, that halide ligated palladium(0) complexes are formed by chemical reduction of $PdX_2(PPh_3)_2$ (X = Cl, Br) by RLi or R_2AlH reagents [15]. The authors pointed out that the structure of the resulting complexes (characterized by ^{31}P-NMR spectroscopy) strongly depends on the halide X and on the chemical reducer, more precisely on the cation accompanying the chemical reducer, suggesting that negatively charged species are formed such as $Li_nX_nPd(0)(PPh_3)_2$ ($n = 1$ or 2). However, the reactivity of these complexes in oxidative additions was too high to be monitored by classical methods such as ^{31}P-NMR spectroscopy. However, since we have just explained that kinetics can be investigated by cyclic voltammetry, the effect of the cation could be examined. The anionic palladium(0) complexes are generated by reduction of $PdCl_2(PPh_3)_2$ in the presence of cations (Li^+, Zn^{2+} introduced, respectively as $LiBF_4$ and $Zn(BF_4)_2$) and the reactivity of the resulting complex with PhI is monitored by cyclic voltammetry as reported above. The oxidative addition is found to be faster in the presence of cations (Table 1). Interaction of the cation with the chloride ligated to the palladium(0) center results in the formation of ion pairs in which a more naked and thus more reactive palladium(0) complex is exposed, being then close to $Pd(0)(PPh_3)_2$, as in compounds **1** and **2**.

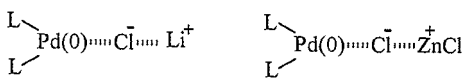

1 **2**

These results show that the structure and the reactivity of the palladium(0) not only depends on the palladium(II) precursor (influence of anions) but also on the way they are generated (influence of cations). Chemical reductions introduce cations and thus more reactive palladium(0) complexes are generated. This stresses out that in a catalytic cycle, presumed innocent ions such as anions (halides released by the aryl halides) or cations (brought by the nucleophiles) may in truth severely interfere in the nature and kinetics of the oxidative addition.

3.2. $Pd(OAc)_2 + nL$ as precursor of $Pd(0)L_2$ ($L = PPh_3$)

A catalytic system often used in Heck reactions (arylation of olefins) consists in mixtures of $Pd(OAc)_2$ and phosphines [1b,c,e–h,j,m]. The palladium(II) salt was usually considered to be reduced in situ to a palladium(0) complex which is then able to activate aryl halides by oxidative addition [3]. However, the reductant and the mechanism of the reduction were unknown.

Cyclic voltammetry performed on mixtures of $Pd(OAc)_2 + 2PPh_3$, in THF and DMF, exhibits initially only the reduction peak of $Pd(OAc)_2(PPh_3)_2$ (Fig. 3a) [16]. However, this complex is not stable as evidenced by the decay of its reduction current as a function of time (Fig. 3a). Simultaneously an oxidation peak appears whose current increases as a function of time (Fig. 3b), showing that a palladium(0) complex is spontaneously generated from $Pd(OAc)_2(PPh_3)_2$. This palladium(0) is not stable when generated in situ from $Pd(OAc)_2 + 2PPh_3$. In order to get and observe more

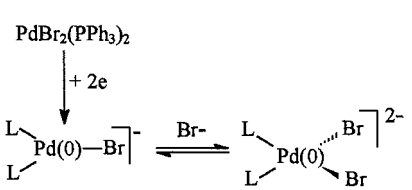

Scheme 3.

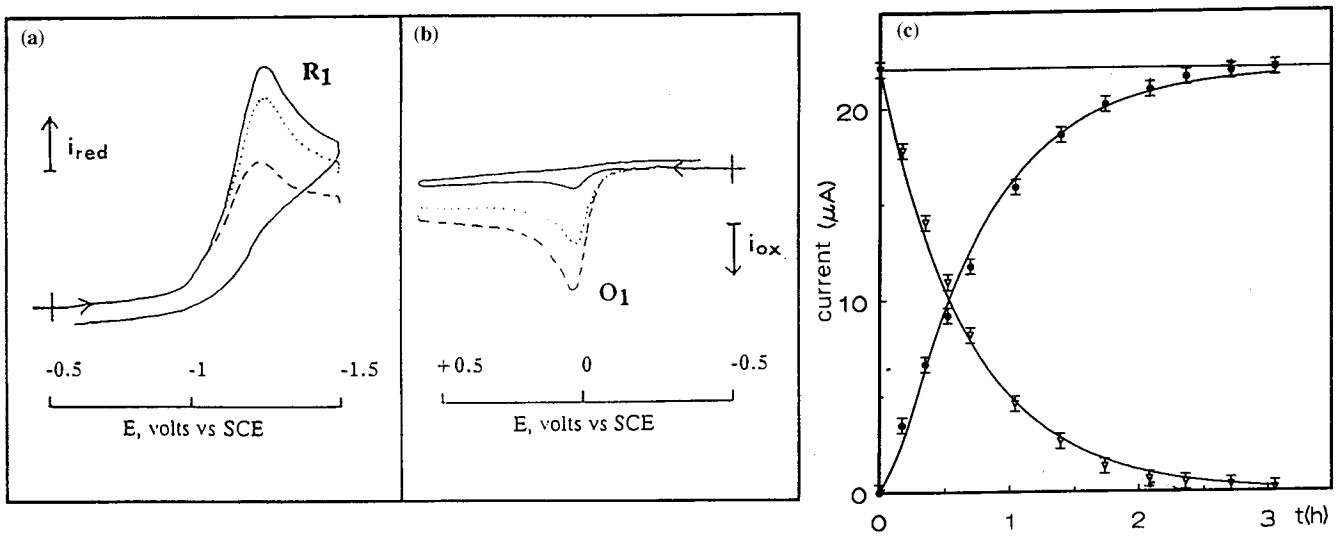

Fig. 3. (a) Cyclic voltammetry of $Pd(OAc)_2$, 2 mmol dm^{-3}, and PPh_3, 4 mmol dm^{-3}, in DMF (containing n-Bu_4NBF_4 0.3 mmol dm^{-3}) at a steady gold disk electrode (i.d. 0.5 mm) with a scan rate of 0.2 V s^{-1}, as a function of time (–) 4, (···) 14, (--) 33 min, 20°C. (b) Cyclic voltammetry of the palladium(0) complex generated in situ from $Pd(OAc)_2$, 2 mmol dm^{-3}, and PPh_3, 4 mmol dm^{-3}, as a function of time, (–) 7, (···) 17, (--) 31 min, 20°C. (c) Variation of the plateau currents at a rotating gold disk electrode (i.d. 2 mm, $\omega = 105$ rad s^{-1}) of a mixture of $Pd(OAc)_2$, 2 mmol dm^{-3} and PPh_3, 20 mmol dm^{-3}, *versus* time. 25°C. (▽) Variation of the reduction current at -1.3 V of $Pd(OAc)_2(PPh_3)_2$. (●) Variation of the oxidation current at $+0.4$ V of the palladium(0) formed in situ. The solid lines are the theoretical predictions according to Eqs. 6 and 8 with $k_1 = 4.2 \times 10^{-4}$ s^{-1} (Eq. (6)) and $k_2 = 1.8 \times 10^{-3}$ s^{-1} (Eq. (8)).

stable complexes, mixture of $Pd(OAc)_2 + nPPh_3$ ($n > 2$) had to be investigated. In the ^{31}P-NMR spectrum of a mixture of $Pd(OAc)_2 + 10PPh_3$, one notices the decay of the signal of $Pd(OAc)_2(PPh_3)_2$ with time and the concomitant growth of a broad signal characteristic of palladium(0) complexes involved in an equilibrium with PPh_3 whose signal as free ligand is never observed. After 2 h only two signals are detected, the broad signal of the palladium(0) complex and the signal of triphenylphosphine oxide $(O)PPh_3$ [16]. Thus, triphenylphosphine reduces the palladium(II) to a palladium(0) complex. Osawa and Hayashi have reported similar NMR experiments performed with $Pd(OAc)_2$ and BINAP ligand. BINAP oxide was then characterized by ^{31}P-NMR spectroscopy together with a palladium(0) complex ligated by BINAP [17].

Since the oxidation peak potential and the ^{31}P-NMR signal of the palladium(0) generated in situ from $Pd(OAc)_2$ and $5PPh_3$ differ from those of $Pd(0)(PPh_3)_4$, AcO^- ions were suspected to play a role. Addition of acetate ions to $Pd(0)(PPh_3)_4$ provokes a shift of its unique but broad ^{31}P-NMR signal, suggesting that acetate ions actually interfere in equilibrium (2) to form anionic species such as $Pd(0)(PPh_3)_n(OAc)^-$ ($n = 2$, 3) which are still involved in a fast equilibrium with the phosphine (Eq. (10)) [18], thus being similar in behavior as halide ions vis a vis palladium(0) complexes (Section 3.1).

By means of a rotating disk electrode polarized on the oxidation wave of the palladium(0) and on the reduction wave of $Pd(OAc)_2(PPh_3)_2$, the evolution of the palladium(0) concentration (proportional to its oxidation current) and that of the palladium(II) precursor (proportional to its reduction current) are monitored as a function of time (Fig. 3c) [19]. The formation of the palladium(0) is first order in palladium and zero order in PPh_3. This means that the rate determining step for the formation of the palladium(0) complex is an intramolecular reduction (Eq. 6) in which PPh_3 reduces the palladium(II) via an inner sphere atom transfer and is oxidized to phosphine oxide through an intermediate phosphonium salt, as in Mitsonobu reactions (Eqs. 6 and 7).

$$Pd(OAc)_2 + 2PPh_3 \overset{fast}{\rightarrow} Pd(OAc)_2(PPh_3)_2 \quad \text{(under mixing)} \tag{5}$$

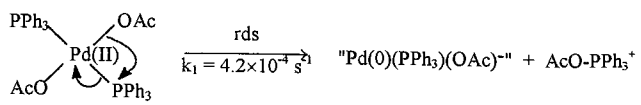

(6)

$$AcO{-}PPh_3^+ + H_2O \rightarrow AcOH + (O)PPh_3 + H^+ \tag{7}$$

$$\text{“}Pd(0)(PPh_3)(OAc)^-\text{”} + PPh_3 \overset{fast}{\rightarrow} Pd(0)(PPh_3)_2(OAc)^- \tag{8}$$

Overall reactions:

$$Pd(OAc)_2 + 3PPh_3 + H_2O \rightarrow Pd(0)(PPh_3)_2(OAc)^- + H^+ + AcOH + (O)PPh_3 \tag{9}$$

$$Pd(0)(PPh_3)_2(OAc)^- + PPh_3 \rightleftarrows Pd(0)(PPh_3)_3(OAc)^- \quad K'_2 \qquad (10)$$

The unstable palladium(0) complex formed in the rate determining step (Eq. 6) is stabilized by fast ligation of excess phosphine (Eqs. (8) and (10)) affording anionic palladium(0) species ligated by acetate ions and phosphines [18,19]. In our experiments with PPh_3, the rate of formation of the palladium(0) is not affected by the presence of water (Table 2 entries 3 and 6) which indicates that water (Eq. (7)) in not involved in the rate determining step of the reaction [19,20].

The spontaneous formation of palladium(0) complexes from mixture of phosphines and palladium(II) salt is not restricted to acetate salts but takes place as soon as an oxygenated ligand is present on the palladium(II) center. Palladium(0) complex are thus generated from $Pd(OCOCF_3)_2$ (Table 2) [21], from $PdCl_2(PPh_3)_2$ in basic medium (through the intermediary of $PdCl(OH)(PPh_3)_2$ as reported by Alper et al. [22]), from cationic complexes such as $[Pd(II)(PPh_3)_2, (BF_4)_2]$ provided water is present [23] (through the formation of $[Pd(II)(OH)(H_2O)(PPh_3)_2, BF_4]$ which becomes the rate determining step of the overall reaction) [24]. The formation of palladium(0) from $Pd(OAc)_2$ is general whatever the phosphine (aromatic [19], aliphatic [19], hydrosoluble such as TPPTS [25] (Table 2)). The rate constant for the formation of palladium(0) complexes from mixtures of $Pd(OAc)_2$ and *para*-substituted triarylphosphines follows a Hammett correlation ($\rho = +2.4$ at 25°C) which means that the formation of the palladium(0) complex is faster when the triarylphosphine is substituted by an electron withdrawing group [19]. We observed a single exception with the tri(*ortho*-tolylphosphine) for which no palladium(0) complex is spontaneously formed from $Pd(OAc)_2$. This abnormal behavior has been then elucidated by Herrmann et al. who have established the formation of a palladacycle in this case [26].

We have established that phosphines are able to reduce $Pd(OAc)_2$ to palladium(0) complexes. However, when involved in a Heck reaction, $Pd(OAc)_2$ has to face reagents other than phosphines, such as bases (NEt_3) or alkenes which have also been suspected to act as reducers. The rate of formation of palladium(0) has therefore been determined in the presence of NEt_3 and 1-decene [19]. From Table 2 (entries 3–5), one deduce that were these reagents able to reduce $Pd(OAc)_2$, the corresponding rates of reduction are much slower than for the triphenylphosphine, since their presence does not affect the reaction.

Table 2
Comparative rate constant k_1 for the formation of Pd(0) as a function of the precursor in DMF at 25°C

No.	Precursor of Pd(0) (2 mmol dm^{-3})	10^4 k_1 (s^{-1})
1	$Pd(OCOCF_3)_2 + 10PPh_3$	50
2	$Pd(OAc)_2 + 10TPPTS$	11
3	$Pd(OAc)_2 + 10PPh_3$	4.2
4	$Pd(OAc)_2 + 10PPh_3 + 50NEt_3$	4.0
5	$Pd(OAc)_2 + 10PPh_3 + 50$(1−decene)	3.9
6	$Pd(OAc)_2 + 10PPh_3 + 10H_2O$	3.9

The kinetics of the oxidative addition of PhI with the palladium(0) generated in situ from mixtures of $Pd(OAc)_2$ and $nPPh_3$ ($n \geq 3$) in DMF is monitored by amperometry at a rotating disk electrode [18]. The potential of the electrode is set at $+0.2$ V *versus* SCE and the decay of the oxidation current of the palladium(0) complex is recorded as a function of time after addition of phenyl iodide. The oxidative addition is slower when the concentration of PPh_3 increases (compare entries 9 and 11 in Table 1) whereas it does not depend on the acetate concentration. This indicates that the reactive species in the oxidative addition is involved in an up-hill equilibrium in which PPh_3 is released but not OAc^- so that the reactive species is the less ligated complex $Pd(0)(PPh_3)_2(OAc)^-$ (Eq. (10), $K'_2 = 5 \times 10^2$ mol^{-1} dm^3). On the basis of these results, the reactivity of $\{Pd(0)(PPh_3)_4 + 1AcO^-\}$ and that of the palladium(0) generated from the mixture $\{Pd(OAc)_2 + 5PPh_3\}$ should be very similar since they formally lead to the same major species in solution: $Pd(0)(PPh_3)_3(OAc)^-$ with one equivalent of PPh_3 in both cases and one equivalent of $(O)PPh_3$ in the second one. Comparison of entries 8 and 9 (Table 1) evidences however a higher and unexpected reactivity for the second system. This unexpected effect can be easily explained by taking in account that protons are formed in the overall formation of palladium(0) from $Pd(OAc)_2$ (Eq. (9)). These protons probably interfere with the acetate of $Pd(0)(PPh_3)_2(OAc)^-$ to form a more naked and thus more reactive complex **3** close to $Pd(0)(PPh_3)_2$.

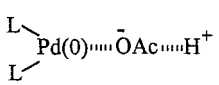

3

The effect of protons would then be extremely similar to that of cations vis-a-vis $Pd(0)(PPh_3)_2Cl^-$, as we report above in Section 3.1 (compare compound **3** to compounds **1** and **2**). This hypothesis could be checked by addition of a base, NEt_3, which by neutralizing the protons, slows down the oxidative addition (compare entries 9 and 10 in Table 1) thus bringing a rate comparable to that of $\{Pd(0)(PPh_3)_4 + 1AcO^-\}$ (compare entries 8 and 10 in Table 1) [18]. Thus, the two systems $\{Pd(0)(PPh_3)_4 + 1AcO^-\}$ and the palladium(0) generated from the mixture $\{Pd(OAc)_2 + 5PPh_3\}$ have the same reactivity provided the protons of the second system are neutralized by a base such as NEt_3 which is often used in Heck procedures.

The mixture $\{Pd(OAc)_2 + 3PPh_3\}$ which leads to the quantitative formation of the most reactive species $Pd(0)(PPh_3)_2(OAc)^-$ is the most reactive system in agreement with the above discussion and a decelerating effect of the base, NEt_3, on the rate of the oxidative addition is again observable (entries 11 and 12 in Table 1). In the absence of any base, the palladium(0) complex generated from $Pd(OAc)_2 + 3PPh_3$, i.e. $[Pd(0)(PPh_3)_2(OAc)^-, H^+]$ is relatively unstable and its stability improves dramatically in the presence of NEt_3. As postulated above, neutralization of protons results in the formation of a complex $Pd(0)(PPh_3)_2(OAc)^-$ more stable than $[Pd(0)(PPh_3)_2(OAc)^-, H^+]$ and thus less reactive in the oxidative addition. The mechanistic consequences of this effect of the base will be discussed later on, when examining the mechanism of the Heck reaction (Section 5.2).

3.3. $Pd(0)(dba)_2 + nL$ as precursor of $Pd(0)L_2$ (dba = trans,trans-dibenzylidenacetone)

The air stable $Pd(0)(dba)_2$ complex associated to monodentate (L) or bidentate (L–L) phosphine affords efficient palladium(0) catalysts [1,c,f,h,j–m,27]. The effective palladium(0) is generated in situ and thus investigation of the role of the ligand in catalytic reaction is made easier than starting from air sensitive $Pd(0)L_4$ complexes. Moreover, the number of phosphine ligand introduced with $Pd(0)(dba)_2$ can be limited to two (for monodentate phosphines) or to one (for bidentate phosphines), a feature of importance when the phosphine is an expensive chiral ligand. In this context, it was implicitly admitted until our work that dba was a very labile ligand and mixtures of $\{Pd(dba)_2 + 2L\}$ and $\{Pd(dba)_2 + 4L\}$ were considered as formally equivalent to $Pd(0)L_2$ and $Pd(0)L_4$, respectively. However, $Pd(PPh_3)_4$ is often more efficient than $\{Pd(dba)_2 + 4PPh_3\}$ and even more efficient than $\{Pd(dba)_2 + 2PPh_3\}$ as evidenced at several occasions in literature [28], suggesting that dba plays a role in catalytic processes. This prompted us to investigate precisely the kinetic role of the innocent ligand dba.

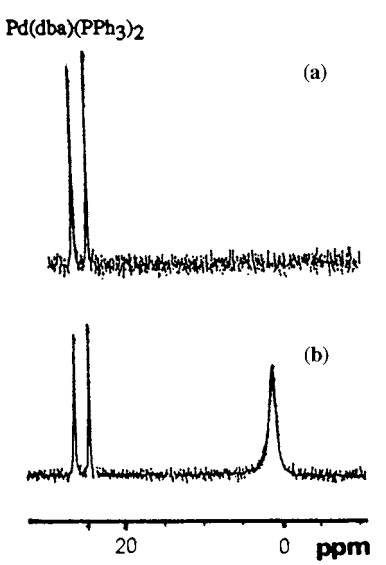

Fig. 4. ^{31}P-NMR spectrum (162 MHz) in 3 ml of THF and 0.2 ml of acetone-d_6 with H_3PO_4 as an external reference. (a) $Pd(dba)_2$ (14 mmol dm^{-3}) + two equivalents of PPh_3. (b) $Pd(dba)_2$ (14 mmol dm^{-3}) + four equivalents of PPh_3.

3.3.1. $Pd(0)(dba)_2 + nL$ ($n \geq 2$, L = monodentate phosphine ligands)

^{1}H-NMR spectra of $Pd(dba)_2$ in chloroform d_1, shows one free and one ligated dba (Eq. (11)). A ^{31}P-NMR spectrum performed on a solution of $Pd(dba)_2$ and $2PPh_3$, in THF or DMF, exhibited two signals of equal amplitude characteristic of two different phosphorous atoms on the palladium(0) center (Fig. 4a) [29]. These signals are assigned to the complex $Pd(dba)(PPh_3)_2$ (Eq. (12)) in which a monoligation of the dba ligand on the palladium induces the presence of two non-equivalent phosphorous atoms [29,30]:

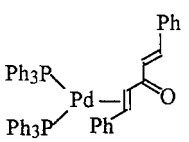

$$Pd(0)(dba)_2 \rightarrow Pd(0)(dba) + dba \quad (11)$$

$$Pd(0)(dba) + 2PPh_3 \rightarrow Pd(0)(dba)(PPh_3)_2 \quad (12)$$

After adjunction of two additional equivalents of PPh_3 the two signals of $Pd(0)(dba)(PPh_3)_2$ are still present but a broad signal appears at upper field (Fig. 4b). Under no circumstances probed in our studies, the free ligand PPh_3 signal is observed. Therefore, the broad upperfield signal characterizes palladium(0) complexes in equilibrium with the ligand PPh_3 (Eq. (13)) (S = solvent).

$$SPd(0)L_3 \leftrightarrows SPd(0)L_2 + L \qquad K_2 = \frac{[SPdL_2][L]}{[SPdL_3]} \quad (13)$$

From these two series of experiments, one readily infers that the mixture $\{Pd(dba)_2 + 2PPh_3\}$ cannot be equivalent to $Pd(0)(PPh_3)_2$ but that the major complex present is $Pd(0)(dba)(PPh_3)_2$. A mixture $\{Pd(dba)_2 + 4PPh_3\}$ affords at least two major complexes, $Pd(0)(dba)(PPh_3)_2$ and $SPd(0)(PPh_3)_3$ [29].

Cyclic voltammograms of $Pd(dba)_2$ (2 mmol dm^{-3}) in the presence of two equivalents of PPh_3, in DMF or THF, (containing n-Bu_4NBF_4, 0.3 mol dm^{-3}) exhibit two oxidation waves O_1 and O_2 (Fig. 5a). The major oxidation peak O_2 characterizes the complex $Pd(dba)(PPh_3)_2$ whereas the plateau-shaped oxidation wave O_1 characterizes the more easily oxidized species, $SPd(PPh_3)_2$ involved in a dynamic equilibrium (CE mechanism [8]) with $Pd(dba)(PPh_3)_2$ (Eq. (14)) [29].

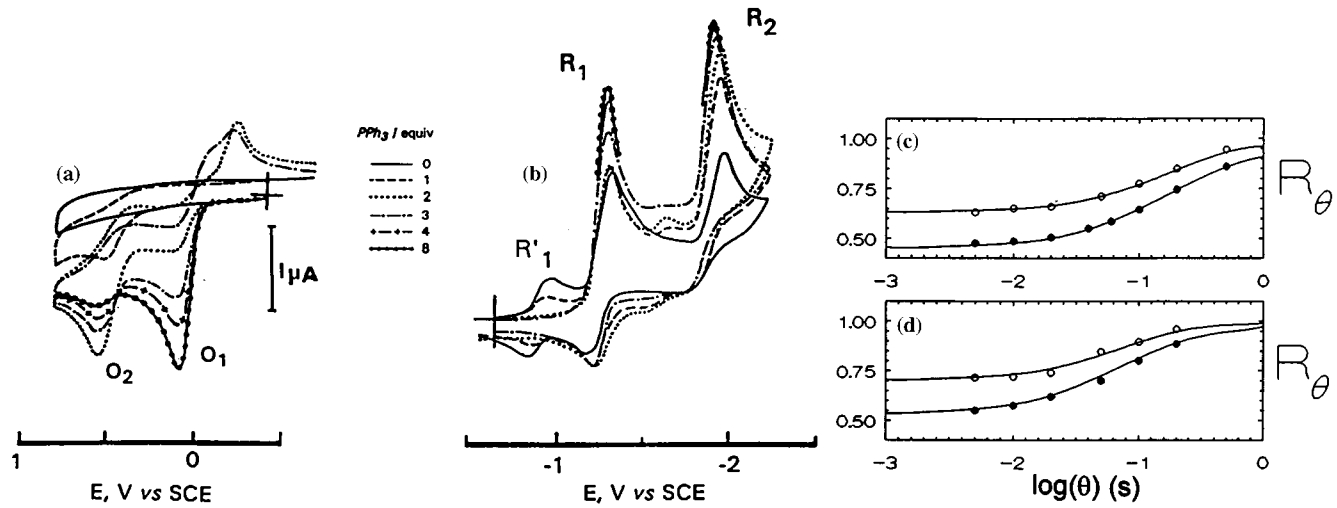

Fig. 5. (a) Cyclic voltammetry performed in DMF (containing n-Bu_4NBF_4, 0.3 mmol dm^{-3}) at a stationary gold disk electrode (0.5 mm diameter) with a scan rate of 0.2 V s^{-1}. Oxidation of $Pd(dba)_2$ (2 mmol dm^{-3}) in the presence of various equivalents n of added PPh_3 as shown in the insert. (b) Reduction of $Pd(dba)_2$ (2 mmol dm^{-3}) in the presence of various equivalents n of added PPh_3 as shown in the insert. (c) Chronoamperometric oxidation of $Pd(dba)_2$ (2 mmol dm^{-3}) in DMF (containing n-Bu_4NBF_4, 0.3 mol dm^{-3}) in the presence of various amounts of added PPh_3, performed at gold disk electrodes (0.5 mm or 25 μm diameter) at 20°C. Variations of $R_\theta = i_{O_1}/(i_{O_1} + i_{O_2})$ as a function of the pulse duration θ and the phosphine concentration: $[PPh_3]_0 = 20$ (●), 40 (○) mmol dm^{-3}. (d) Same chronoamperometric experiment in THF.

$$\underset{O_2}{Pd(0)(dba)L_2} + S \rightleftarrows \underset{O_1}{SPd(0)L_2} + dba$$

$$K_1 = \frac{[SPdL_2][dba]}{[Pd(dba)L_2]} \qquad (14)$$

Upon increasing PPh_3 concentration, wave O_1 becomes peak-shaped and increases at the expense of that of O_2 (Fig. 5a). Simultaneously, dba is released in solution as attested by the increase of its two reduction peak currents at R_1 and R_2 (Fig. 5b). This demonstrates that complexes $Pd(0)(dba)(PPh_3)_2$ and $SPd(0)(PPh_3)_3$ are involved in a second equilibrium involving now the phosphine ligand (Eq. (15)) [31].

$$\underset{O_2}{Pd(0)(dba)L_2} + L \rightleftarrows \underset{O_1}{SPd(0)L_3} + dba$$

$$K_0 = \frac{[SPdL_3][dba]}{[Pd(dba)L_2[L]]} \qquad (15)$$

The value of the equilibrium constant K_0 between $Pd(dba)(PPh_3)_2$ and $SPd(PPh_3)_3$ (Eq. (15)) has been determined by chronoamperometry. In cyclic voltammetry, for a given concentration of PPh_3, the ratio i_{O_1}/i_{O_2} of the oxidation currents of O_2 and O_1 decreases when the scan rate increases, i.e. when the time scale decreases. This behavior is characteristic of a CE mechanism involving two species in equilibrium, as in Eq. (15). The oxidation peak currents (usually proportional to the concentrations) are then not representative of the concentrations of the two complexes in the bulk solution but of the dynamic concentrations resulting from the shifting of the equilibrium (Eq. (15)) towards the most easily oxidized species, i.e. to its right hand, by the continuous oxidation of $SPd(PPh_3)_3$ in the diffusion layer. For shorter and shorter time scales (i.e. larger scan rates), the equilibrium (Eq. (15)) is less and less shifted to the right by the oxidation of $SPd(PPh_3)_3$ until the equilibrium is frozen. The oxidation currents are determined by chronoamperometry which allows, in this case, more precise measurements than by cyclic voltammetry. The oxidation currents i_{O_1} and $i_{O_1} + i_{O_2}$ are measured by performing two series of potential steps of same duration θ, one on O_1 and the other one on O_2. The ratio $R_\theta = i_{O_1}/(i_{O_1} + i_{O_2})$ is plotted *versus* the time scale θ of the chronoamperometric experiments and exhibits a plateau at short θ values in which the equilibrium is kinetically frozen (Fig. 5c–d). The equilibrium constant K_0 is then available from the value of this plateau (Table 3) [29].

The complex $Pd(0)(dba)(PPh_3)_2$ is also characterized in UV spectroscopy through observation of its absorption band at $\lambda_{max} = 396$ nm, in DMF (Fig. 6) [32,33]. This absorption band progressively disappears when PPh_3 is progressively added to the solution and com-

Table 3
Determination of the equilibrium constant K_0 by different techniques at 20°C[a]

Technique	K_0	
	DMF	THF
Chronoamperometry	0.16 ± 0.02	0.23 ± 0.03
UV spectroscopy	0.16 ± 0.02	n.d.
Kinetics of the oxidative addition by steady state amperometry	0.140 ± 0.015	0.232 ± 0.007

[a] $Pd(0)(dba)(PPh_3)_2 + PPh_3 + S \leftrightarrows SPd(0)(PPh_3)_3 + dba$ $K_0(15)$.

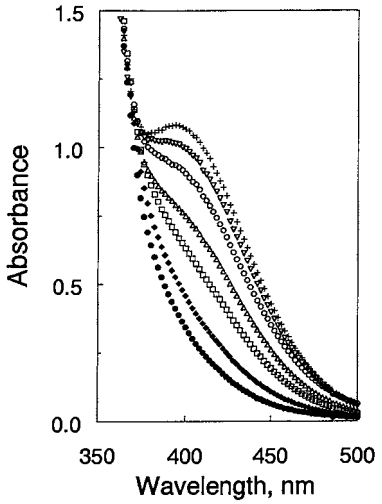

Fig. 6. UV spectroscopy performed in DMF in a 1 mm path cell at 20°C. $Pd(dba)_2$ (0.1 mmol dm^{-3}) $+ nPPh_3$. $n = 2$ (+), 4 (▽), 6 (○), 10 (△), 20 (□), 50 (◆), 100 (●) equivalents.

pletely disappears when at least 50 equivalents of PPh_3 are added to $Pd(dba)(PPh_3)_2$ (Fig. 6). This means that at least 50 equivalents of PPh_3 are necessary to completely displace dba from $Pd(dba)(PPh_3)_2$. Thus, dba in $Pd(dba)(PPh_3)_2$ is not as labile as usually postulated. K_0 can be determined by UV spectroscopy and calculated from the ratio $x = (D_0 - D_{eq})/(D_0 - D_\infty)$ (D_0, initial absorbance of $Pd(0)(dba)(PPh_3)_2$, at $\lambda = 450$ nm; D_{eq}, absorbance at the equilibrium position for a given value of n (equivalent of PPh_3); D_∞, absorbance when the equilibrium is totally shifted to its right-hand side) (Table 3) [32]: $K_0 = x(1+x)/(1-x)(n-2-x)$.

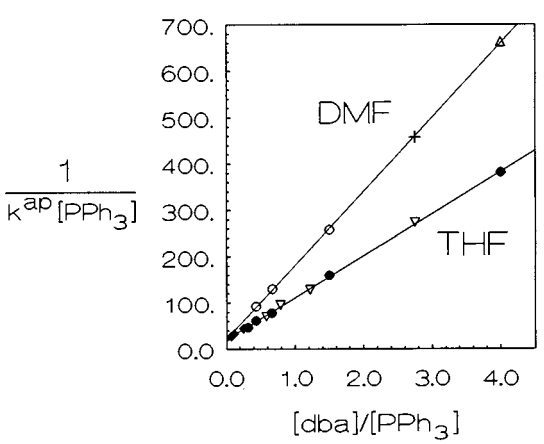

Fig. 7. Variations of the apparent rate constant, k^{ap} ($M^{-1}\ s^{-1}$) of the oxidative addition of PhI (5–20 equivalents) with the palladium(0) generated from mixtures of $Pd(dba)_2$ (2 mmol dm^{-3}), dba and PPh_3, as a function of dba and PPh_3 concentrations, in DMF and THF (containing n-Bu_4NBF_4, 0.3 mol dm^{-3}). Initial concentration of $Pd(dba)_2$: 2 mmol dm^{-3}; concentration of added PPh_3: 10–80 mmol dm^{-3}; concentration of added dba: 0 (●), 20 (▽), 40 (◆) mmol dm^{-3} in THF and 20 (○), 40 (+), 60 (△) mmol dm^{-3} in DMF 20°C.

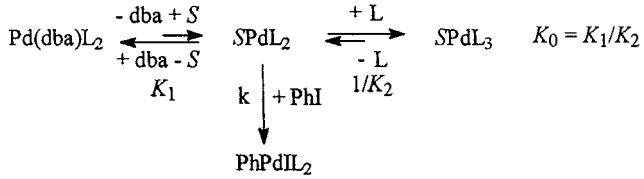

Scheme 4.

A third route for the determination of K_0 is afforded by kinetic investigation of the reactivity of mixtures of $Pd(dba)_2 + nPPh_3$ ($n \geq 2$) in oxidative addition with phenyl iodide [29]. A rotating disk electrode is polarized on the plateau of waves O_1 ($SPd(PPh_3)_3$) or O_2 ($Pd(dba)(PPh_3)_2$) and the decay of the oxidation current, featuring that of all palladium(0) complexes, is recorded as a function of time, after addition of PhI. The overall rate of the oxidative addition follows a kinetic law first order in PhI and first order in palladium(0) and is slower when the concentration of the phosphine and/or the concentration of dba increase (Fig. 7) [34]. The reactive species is the lowest ligated complex $SPd(PPh_3)_2$ involved in a fully dynamic equilibrium with the mains species $SPd(PPh_3)_3$ and $Pd(dba)(PPh_3)_2$ as in Scheme 4.

The kinetic law corresponding to the mechanistic Scheme 4 is first order as observed, with an apparent rate constant given by:

$$k_{app} = \frac{k}{1 + [dba]/K_1 + [PPh_3]/K_2} \quad \text{i.e.}$$

$$\frac{1}{k_{app}[PPh_3]} = \left\{\frac{1}{k[PPh_3]} + \frac{1}{kK_2}\right\} + \frac{[dba]}{kK_1[PPh_3]}$$

which fits the experimental data (Fig. 7). The experimental intercept of the linear regression does not depend on $[PPh_3]$ which means that $1/k[PPh_3]$ is much smaller than $1/kK_2$, so that only kK_2 can be determined from the intercept. kK_1 is determined from the slope and K_0 from the ratio of these two values (Table 3) [29].

Determination of K_0 by three independent techniques results in similar values (Table 3). Interestingly, two of these methods (chronoamperometry and kinetics) involve conditions in which ionic strength is high (supporting electrolyte: n-Bu_4NBF_4, 0.3 mol dm^{-3}) while the third one (UV) involves low ionic strength (no salt added). Thus the good coherence between the three sets of values in Table 3 demonstrates that ionic strength has no effect on this equilibrium. Whatever the solvent, the value of K_0 is less than unity which shows that for comparable overall dba and PPh_3 concentrations (i.e. as in usual procedures), the overall equilibrium (15) is in favor of $Pd(dba)(PPh_3)_2$. This is then the major complex in solution, whereas the reactive species in the oxidative addition, $SPd(PPh_3)_2$ is present as traces. Consequently, the following order of reactivity is established in THF and DMF (Table 1) [29]:

$Pd(PPh_3)_4 > \{Pd(dba)_2 + 2PPh_3\} > \{Pd(dba)_2 + 4PPh_3\}$

which definitively demonstrates that $\{Pd(dba)_2 + 2PPh_3\}$ is by no way equivalent to $Pd(PPh_3)_2$ and $\{Pd(dba)_2 + 4PPh_3\}$ to $Pd(PPh_3)_4$ as usually admitted. These kinetic findings and quantitative data cast therefore light on many puzzling results reported in literature [28].

3.3.2. Mixtures of $Pd(dba)_2 + n(p\text{-}Z\text{-}C_6H_4)_3P$ ($n \geq 2$)

Mixtures of $Pd(dba)_2$ and nL (L = *para*-*Z*-substituted triphenylphosphines, $n \geq 2$) in DMF and THF, lead to the formation of $Pd(dba)L_2$ and $SPdL_3$ in equilibrium with $SPdL_2$ (Scheme 4) [32]. For a given value of n, the equilibrium between $Pd(dba)L_2$ and $SPdL_3$ (Eq. (15), constant K_0^Z) lies more in favor of $SPdL_3$ when the phosphine is less electron rich (Hammett correlation for K_0^Z with $\rho = +4$). For comparable cone angles, the release of dba from $Pd(dba)L_2$ to form $SPdL_3$ is easier and easier when the phosphine becomes less and less electron rich.

Whatever Z, the less ligated complex transient species $SPdL_2$ remains the only reactive one in the oxidative addition with phenyl iodide (Scheme 4). It is generally admitted that the oxidative addition is sensitive to electronic factors: it is faster when the phosphine is more electron rich. In contrast with this spread knowledge, when the palladium(0) complex is generated from mixtures of $Pd(dba)_2$ and nL (L = *para*-*Z*-substituted triphenylphosphines, $n \geq 2$), the oxidative addition does not follow a monotonous correlation. Instead, bell shaped curves are obtained with a maximum whose value and position depend on n, i.e. on the phosphine concentration (Fig. 8) [32]. As evidenced by these studies, the overall reactivity in the oxidative addition is governed by two factors: (i) the intrinsic reactivity of $SPdL_2$ in the oxidative addition expressed by k^Z (Scheme 4) and (ii) the concentration of $SPdL_2$ which is controlled by the values of the equilibrium constants K_1^Z and K_0^Z. When the phosphine becomes more electron rich, the complex $SPdL_2$ becomes more nucleophilic and k^Z increases. But its concentration decreases because the equilibrium constants K_1^Z and K_0^Z decrease and the equilibria (14) and (15) shift more in favor of $Pd(dba)L_2$. As a results of these two antagonist effects, bell shaped curves are obtained.

3.3.3. Mixtures of $Pd(dba)_2 + nTFP$ ($n \geq 2$, *TPF = tri-2-furylphosphine*)

The tri-2-furylphosphine ligand TFP, has been recently introduced as ligand in palladium(0)-catalyzed reactions [35a] and found to be very often more efficient than PPh_3. The kinetics of the oxidative addition has been investigated and compared to that involving PPh_3.

The determination of the equilibrium constant K_0 between $Pd(dba)(TFP)_2$ and $SPd(TFP)_3$ (Eq. (15)) shows that whatever the solvent, THF or DMF, $K_0^{TFP} > K_0^{PPh3}$ [33]. Thus, the displacement of dba from the complex $Pd(dba)L_2$ to form $SPdL_3$ is easier for TFP than for PPh_3. Since TPF is less basic than PPh_3, the effect of the basicity on the value of K_0 is consistent with the trend evidenced in the case of *para*-substituted phosphines (see above).

Reactivities of mixtures of $Pd(dba)_2 + nTFP$ have been compared to those of $Pd(dba)_2 + nPPh_3$, as a function of n, in oxidative addition with phenyl iodide. In DMF, the mixture $\{Pd(dba)_2 + nTFP\}$ was more reactive than $\{Pd(dba)_2 + nPPh_3\}$ whatever n ($n \geq 2$). In THF, the mixture $\{Pd(dba)_2 + nTFP\}$ was less reactive than $\{Pd(dba)_2 + nPPh_3\}$ when $n = 2$ or 4, whereas the reverse order of reactivity was observed when $n > 6$ (Fig. 9) [33]. Thus, in THF, the order of reactivity strongly depends on the value of n. This behavior is easily rationalized within the framework established

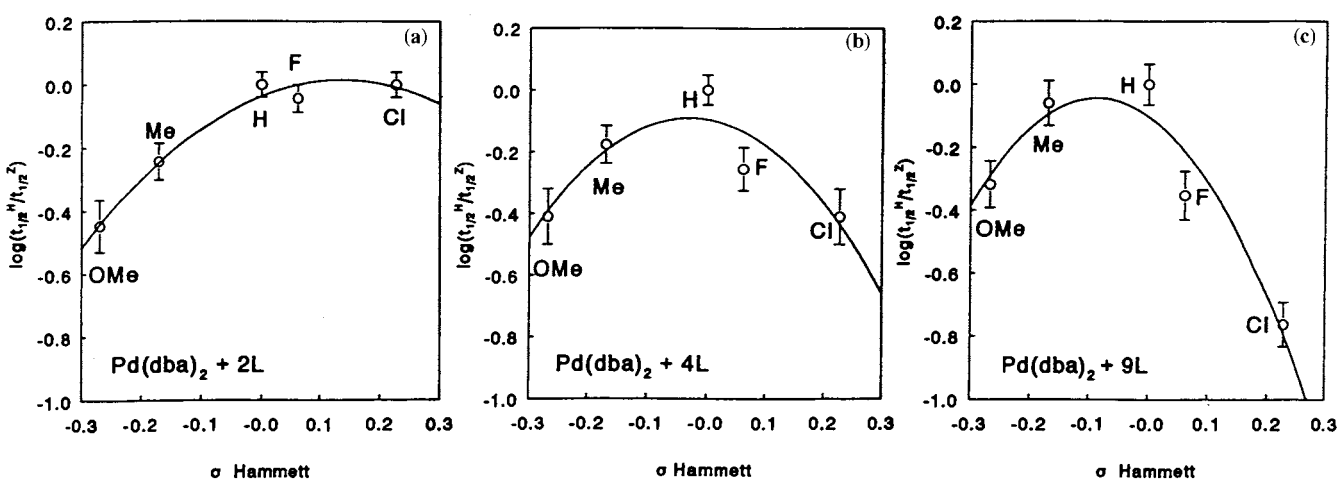

Fig. 8. Hammett plot for the oxidative addition of PhI with the palladium(0) generated in situ in mixtures of $Pd(dba)_2$ and n (p-Z-$C_6H_4)_3P$ in DMF at 20°C. $[Pd(dba)_2] = 2$ mmol dm^{-3}; $[PhI] = 10$ mmol dm^{-3}. (a) $n = 2$. (b) $n = 4$. (c) $n = 9$.

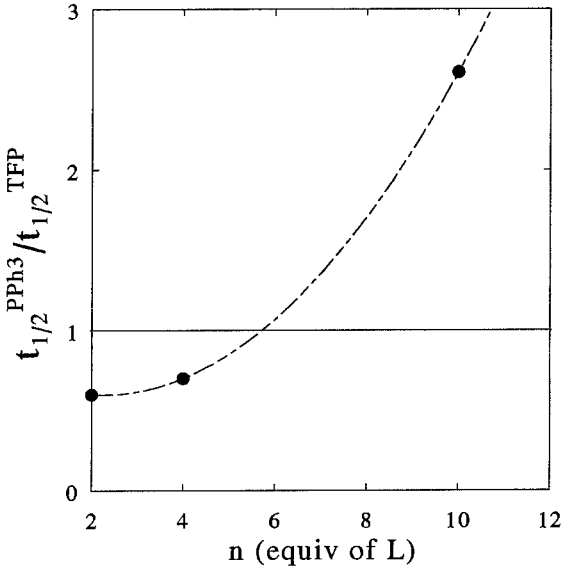

Fig. 9. Kinetics of the oxidative addition of PhI (2 mmol dm^{-3}) with the palladium(0) complex generated in situ from mixture of $Pd(dba)_2$ (2 mmol dm^{-3}) $+n$TFP ($n=2$, 4, ten equivalents) and from $Pd(dba)_2$ (2 mmol dm^{-3}) $+n PPh_3$ ($n=2$, 4, ten equivalents) in THF (containing n-Bu_4NBF_4, 0.3 mol dm^{-3}) at 20°C. Plot of the ratio $t_{1/2}^{PPh3}/t_{1/2}^{TFP}$ as a function of n.

above for *para*-substituted phosphines, by the involvement of two antagonist effects in the overall reactivity. When $n=2$, $k^{PPh3}K_1^{PPh3} > k^{TFP}K_1^{TFP}$ and only equilibrium (14) is involved. Since TFP is less basic than PPh_3, the intrinsic rate constant of the oxidative addition respects the order: $k^{PPh3} > k^{TFP}$. Conversely, since $K_1^{PPh3} < K_1^{TFP}$, under comparable conditions, the available concentration of $SPd(PPh_3)_2$ is less than that of $SPd(TFP)_2$. As a consequence of these two antagonist effects, PPh_3 results in a more reactive system than TFP showing that k^{PPh3} is considerably higher than k^{TFP}. For higher values of n, ($n>2$) the equilibrium K_0 has to be taken into consideration with $K_0^{PPh3} < K_0^{TFP}$. Thus even if $SPd(TFP)_2$ remains intrinsically less reactive than $SPd(PPh_3)_2$, its concentration becomes considerably higher than that of $SPd(PPh_3)_2$ when n is large, resulting in a higher overall reactivity for the TFP ligand.

In synthetic conditions, in THF, mixtures of $Pd(dba)_2 + n$TFP are used as catalysts for small values of n ($n=2$ or 4). As seen above, the use of TFP instead of PPh_3 results in slower oxidative additions. Consequently, the beneficial effect observed with TFP in catalytic reactions does not originate from the oxidative addition step which is then not the rate determining step of the catalytic cycle but certainly from faster nucleophilic attacks (or transmetallation) [35b] on the arylpalladium(II) complexes formed in the oxidative addition. Indeed, these complexes are expected to be more electron deficient when ligated by TFP than by PPh_3.

3.3.4. Mixtures of $Pd(dba)_2 + n(L–L)$ ($n=1,2$; $L–L$ = bidentate phosphine ligands)

Chiral bidentate phosphine ligands are often used in palladium-catalyzed reactions. In order to understand the crucial role of the ligand in asymmetric inductions, it is worth to characterize the palladium(0) complex(es) active in oxidative additions, just in case this reaction were responsible of the enantioselectivity. Oxidative addition of PhI (although not chiral) with palladium(0) complexes generated in situ in mixtures of $Pd(dba)_2$ and bidentate phosphines allows an easy identification of the major complex in solution and the reactive species as well.

Mixtures of $Pd(dba)_2 + 2L–L$ (where L–L is a bidentate ligand such as dppm, dppe, dppp, dppb, dppf and DIOP) lead to the formation of $Pd(L–L)_2$ complexes which do not undergo oxidative addition with phenyl iodide at room temperature, within all the time scales investigated (ca. few hours) [36].

$$Pd(dba)_2 + 2L–L \rightarrow Pd(L–L)_2 + 2dba \quad (16)$$

$$Pd(L–L)_2 + PhI — \times \rightarrow \cdots \quad (17)$$

Unexpectedly, vis-a-vis common knowledge, a mixture of $Pd(dba)_2 + 2$BINAP does not afford $Pd(BINAP)_2$ but instead Pd(dba)(BINAP) is formed which reacts with PhI.

$$Pd(dba)_2 + 2BINAP \rightarrow Pd(dba)(BINAP) + dba + BINAP \quad (18)$$

Only mixtures of $Pd(dba)_2$ associated with one equivalent of bidentate ligand L–L are therefore of catalytic interest in terms of reactivity in oxidative addition with phenyl iodide. Mixtures of $Pd(dba)_2 + 1L–L$ affords Pd(dba)(L–L) as the major complex (Eq. (19)) [36].

$$Pd(dba)_2 + L–L \rightarrow Pd(dba)(L–L) + dba \quad (19)$$

The structure of Pd(dba)(L–L) complexes established by ^{31}P-NMR spectroscopy for L–L = dppm, dppb, dppf, DIOP, BINAP [36], dppe, dppp [36,30] or by X-ray spectroscopy for L–L = dppe [30], obeys the general formula:

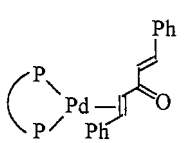

Whatever the ligand, dppf, DIOP or BINAP, the oxidative addition with phenyl iodide is slower in the presence of excess dba, showing that the reactive complex SPd(L–L) is involved in an endergonic equilibrium with the major complex Pd(dba)(L–L) and dba (Eq. 20). However, the reaction order in PhI differs from unity (Fig. 10) which is shown to the fact that Pd(dba)(L–L), although less reactive than SPd(L–L), also reacts with phenyl iodide (Table 4, Scheme 5) [36].

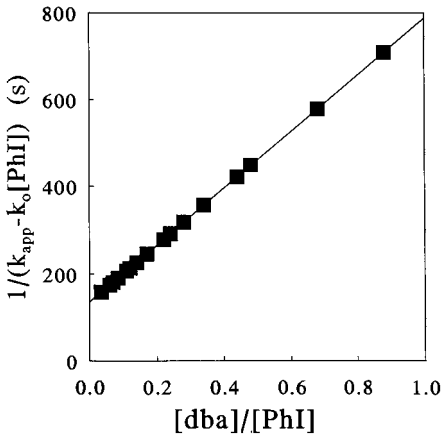

Fig. 10. Kinetics of the oxidative addition of PhI with the palladium(0) complex generated in situ in the mixture of $Pd(dba)_2$ (2 mmol dm^{-3}) + one equivalent of DIOP, in THF at 40°C. Variation of $1/(k_{app} - k_0[PhI])$ *versus* the ratio [dba]/[PhI].

The following order of reactivity has been observed in THF (Table 4) [36]:$\{Pd(dba)_2 + 2PPh_3\} \gg \{Pd(dba)_2 + 1DIOP\} > \{Pd(dba)_2 + 1dppf\} \gg \{Pd(dba)_2 + 1BINAP\}$. One generally considers that the more basic the phosphine and the smaller its angle P–Pd–P, the faster is the oxidative addition. Despite the fact that DIOP is the most basic ligand and BINAP possesses the smallest bite angle, PPh_3 reveals to be involved into the fastest oxidative addition. This shows that thermodynamic factors which control the available concentration of the most reactive species SPd(L–L) or $SPdL_2$ are predominant and that under similar conditions, the concentration of $SPd(PPh_3)_2$ is always considerably higher than that of SPd(L–L) (L–L = DIOP, dppf or BINAP).

In conclusion, whatever the phosphine ligand, monodentate (L) or bidentate (L–L), mixtures of $Pd(dba)_2$ and *n* equivalents of phosphines result in the formation of stable complexes $Pd(dba)L_2$ or Pd(dba)(L–L) ($n = 1$) which are the major complexes in solution [37]. These complexes release dba through an equilibrium which controls the concentration of the less ligated complexes $SPdL_2$ or SPd(L–L) which are the most reactive species in oxidative addition with phenyl iodide. Whereas $Pd(dba)L_2$ does not react in the oxidative addition with PhI, Pd(dba)(L–L) reacts albeit more slowly than SPd(L–L). Thus, the dba ligand plays a crucial role, since it is always present in the major but less reactive complex $Pd(dba)L_2$ or Pd(dba)(L–L) and thus controls the concentration of the dba-free most reactive species. Intrinsic reactivity and concentration of the reactive species may have antagonist effects and as a result, non-linear Hammett correlations are observed when the oxidative addition rate is plotted *versus* the basicity of the phosphine, for monodentate ligands.

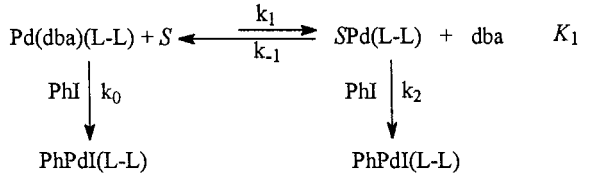

Scheme 5.

As a conclusion, dba in not a labile and innocent ligand as usually considered. Moreover for bidentate ligands, both Pd(dba)(L–L) and SPd(L–L) are reactive. In the presence of a prochiral substrate, a chiral recognition is expected to differ in Pd(dba)(L–L) and Pd(L–L). Since the relative concentration of the two reactive palladium(0) complexes varies with the dba and $Pd(dba)_2$ concentration, the overall asymmetric induction might vary with the experimental conditions whenever the oxidative addition step controls or is part of the chiral induction.

3.4. Conclusion

Although in almost every case, the reactive species in oxidative addition is a palladium(0) complex ligated by two monodentate phosphines L (or one bidentate phosphine, L–L), the overall reactivity is very dependent on the precursor of the palladium(0) complex, as established in Tables 1 and 4. This a priori surprising observation arises from the fact that the reactive palladium(0) complex is often present at low transient concentration because it is involved in endergonic equilibria with the major but unreactive palladium(0) complex, ligated by phosphine or dba. Anions (halides, acetate ions) play a similar role. Both structure and reactivity of palladium(0) complex are strongly affected by the anions which are present on the palladium(II) precursors and are formally available when the anionic palladium(0) complexes are produced. In the following,

Table 4
Comparative reactivity of palladium(0) complexes in the oxidative addition with phenyl iodide in THF, as a function of the ligand at 20°C

No.	Precursor of Pd(0) (2 mmol dm^{-3})	T (°C)	PhI (mol dm^{-3})	$t_{1/2}$ (s)	k_2/k_0	Bite angle P–Pd–P, θ (°)
1	$Pd(dba)_2 + 2PPh_3$	20	0.01	20	–	–
2	$Pd(dba)_2 + 1DIOP$	40	0.2	34	>600	95.48
3	$Pd(dba)_2 + 1dppf$	40	0.2	110	>1000	99.07
4	$Pd(dba)_2 + 1BINAP$	40	0.2	16300	>400	92.69

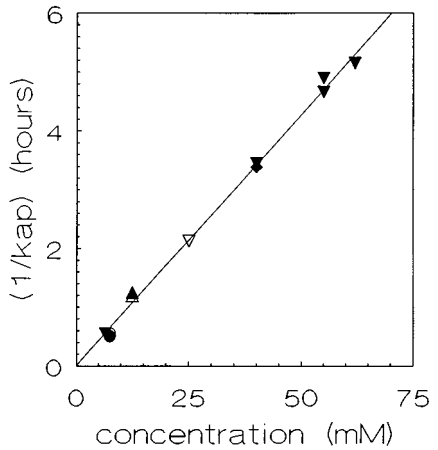

Fig. 11. Oxidative addition of PhI (ten equivalents) with the palladium(0) complex generated by the 2-electron reduction of $PdCl_2(PPh_3)_2$ (concentration C^0) in THF (containing n-Bu_4NBF_4, 0.3 mol dm^{-3}): variation of the apparent rate constant k^{ap} for the transformation of the anionic pentacoordinated $PhPdICl(PPh_3)_2^-$ complex (formed as the primary intermediate in the oxidative addition) into the *trans* complex $PhPdI(PPh_3)_2$ as a function of C^0 (the variation of C^0 induces a variation of the concentration of chloride ions released by the electrochemical reduction of $PdCl_2(PPh_3)_2$). $C^0 = (\bigcirc, \bullet)$ 7.5, $(\triangle)$ 12.2, $(\triangledown)$ 25 and $(\blacklozenge)$ 40 mmol dm^{-3}.

we will describe how these anionic palladium(0) complexes condition the structure and reactivity of the arylpalladium(II) complexes formed in oxidative addition with aryl halides.

4. Structure of the arylpalladium(II) complexes formed in oxidative addition with aryl halides as a function of the precursors of the palladium(0) catalysts

4.1. Pentacoordinated anionic complexes: $ArPdXX'L_2^-$ (X and X′ = halide)

^{31}P-NMR investigation of the oxidative addition of PhI performed from the electrogenerated complex $Pd(0)(PPh_3)_2Cl^-$ (see Section 3.1) in THF shows two singlets [38]. One corresponds to the expected *trans* $PhPdI(PPh_3)_2$ complex and its magnitude increases with time. The second one, initially the main signal, corresponds to a transient species which disappears as a function of time to afford the *trans* $PhPdI(PPh_3)_2$. Upon addition of chloride ions, the *trans* $PhPdI(PPh_3)_2$ is even smaller and its rate of formation becomes slower. Whereas the *trans* $PhPdI(PPh_3)_2$ complex is not oxidized electrochemically, the intermediate complex exhibits an oxidation peak O_2 (Fig. 1b) in voltammetry and its oxidation peak current increases with the chloride ions concentration [38].

It is thus concluded that the *trans* $PhPdI(PPh_3)_2$ complex is not the primary reaction product but that it is formed via evolution of an intermediate complex detected in cyclic voltammetry and ^{31}P-NMR spectroscopy, with a kinetics which is slower in the presence of chloride ions (Fig. 11). Voltammetric measurements prove that the oxidation peak potential of the primary product of the oxidative addition depends on the nature of the aryl moiety, on the halide borne initially by the aromatic halide and on the phosphine. This shows that all these fragments coordinate the palladium(II) center. In addition, titration experiments with $AgNO_3$ show that this transient complex contains one chloride ion. This intermediate complex is therefore an anionic pentacoordinated species $ArPdXClL_2^-$. It slowly affords the *trans* $PhPdI(PPh_3)_2$ through an up-hill equilibrium in which the chloride ion is released as indicated in Scheme 6 ($[Pd(II)] = 2$ mmol dm^{-3}, S = THF) [38].

These results stress the important role of the chloride ions borne by the palladium(0) involved in the oxidative addition since the chloride concentration controls the rate of formation of the *trans* $PhPdI(PPh_3)_2$ complex as well as the existence and concentration of the intermediate pentacoordinated complexes, potentially reactive with nucleophiles (see Section 5.1). Similar pentacoordinated anionic species have also been observed in palladium acetate catalysts (See Section 5.2) yet being much more frangible in the latter case.

4.2. Neutral complexes: $ArPd(OAc)L_2$

The palladium(0) generated in situ from a mixture of $Pd(OAc)_2 + 3PPh_3$ is an anionic species ligated by one acetate ion: $Pd(0)(PPh_3)_2(OAc)^-$ (Section 4.2). Analysis of the complexes formed in its oxidative addition with PhI in THF and DMF, by ^{31}P-NMR spectroscopy,

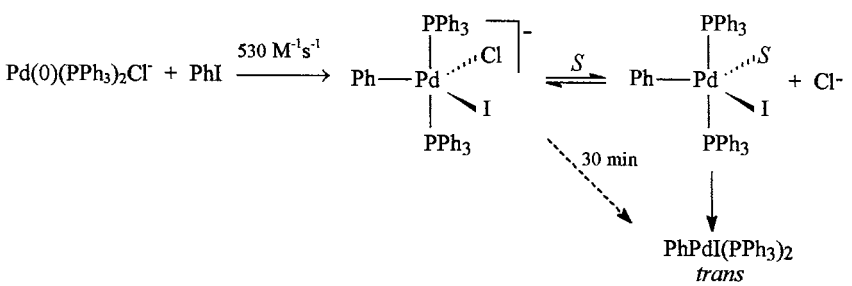

Scheme 6.

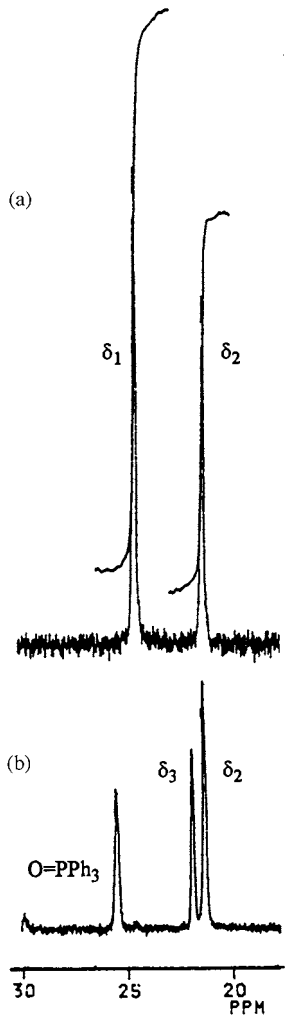

Fig. 12. ^{31}P-NMR spectrum (162 MHz) in 3 ml of DMF and 0.2 ml of acetone-d_6 with H_3PO_4 as an external reference. (a) Mixture of *trans* $PhPdI(PPh_3)_2$ and 1.5 equivalents of nBu_4NOAc. δ_1: *trans* $PhPdI(PPh_3)_2$; δ_2: *trans* $PhPd(OAc)(PPh_3)_2$. (b) Solution resulting from the oxidative addition of PhI (1 equivalent) to the palladium(0) complex generated in situ from the mixture $Pd(OAc)_2$ and $4PPh_3$. The ^{31}P-NMR signal at 25.43 ppm is that of the triphenylphosphine oxide that has been generated together with the palladium(0) complex. δ_2: *trans* $PhPd(OAc)(PPh_3)_2$. δ_3: *trans* $PhPd(PPh_3)_2(DMF)^+$.

shows that the reaction does not afford the expected complex $PhPdI(PPh_3)_2$, as postulated in literature, but a new complex identified as *trans* $PhPd(OAc)(PPh_3)_2$ (Fig. 12b) by comparison with the authentic sample synthesized by reacting AgOAc with *trans* $PhPdI(PPh_3)_2$ [18,19].

$$\{Pd(OAc)_2 + 3PPh_3\} \rightarrow \rightarrow Pd(0)(PPh_3)_2(OAc)^- \quad (21)$$

$$Pd(0)(PPh_3)_2(OAc)^- + PhI \rightarrow PhPd(OAc)(PPh_3)_2 + I^- \quad (22)$$

Analysis of the complexes formed in the oxidative addition by ^{31}P-NMR spectroscopy, shows an extra signal δ_3, beside the signal δ_2 of the *trans* $PhPd(OAc)(PPh_3)_2$ (Fig. 12b). This extra signal is readily assigned to the cationic complex $PhPd(PPh_3)_2^+$ by comparison with an authentic sample synthesized by reacting $AgBF_4$ with *trans* $PhPdI(PPh_3)_2$. In the presence of an excess of added AcO^- ions (introduced as n-Bu_4NOAc), the signal of the neutral complex increases at the expense of that of the cationic complex, evidencing the occurrence of the equilibrium (23) [18].

$$PhPd(OAc)(PPh_3)_2 \leftrightarrows PhPd(PPh_3)_2^+ + AcO^- \quad (23)$$

Also, addition of acetate ions to solutions of *trans* $PhPdX(PPh_3)_2$ (X = Cl, Br, I) provides *trans* $PhPd(OAc)(PPh_3)_2$ via nucleophilic substitution of the halide by the acetate ion (Fig. 12a) (Eq. (24)) [18,39]. These reactions are equilibrated and the equilibrium constants have been calculated from NMR data (Table 5) [18].

$$PhPdX(PPh_3)_2 + AcO^- \rightleftharpoons PhPd(OAc)(PPh_3)_2 + X^- \quad K$$

$$K = \frac{[PhPd(OAc)(PPh_3)_2][X^-]}{[PhPdX(PPh_3)_2][AcO^-]} \quad (24)$$

The detailed mechanism of reaction (22) has been investigated by amperometry [18]. The rotating disk electrode is polarized at +0.2 V *versus* SCE on the plateau of the oxidation wave of $Pd(0)(PPh_3)_2(OAc)^-$. Addition of one equivalent of PhI results in a decay of the oxidation current as a function of time and provides kinetic data on the rate of the oxidative addition (see Section 3.2). However when the electrode is polarized farther on the plateau of the oxidation wave of $Pd(0)(PPh_3)_2(OAc)^-$, i.e. at 0.4 V, the oxidation current first decreases and then increases again (Fig. 13a). The decreasing section is identical to that observed when the electrode potential is set at 0.2 V, showing that the continuous disappearance of the anionic $Pd(0)(PPh_3)_2(OAc)^-$ is still observed as the first step of the overall reaction. The later and increasing section corresponds to the oxidation current of iodide ions which are slowly released in solution after completion of the first step of the oxidative addition. Thus the formation of $PhPd(OAc)(PPh_3)_2$ in the oxidative addition proceeds in two separated steps as in Scheme 7 ($[Pd(II)] = 2$ mmol dm^{-3}) and proceeds therefore again

Table 5
Equilibrium constant K at 27°C[a]

X	K	
	DMF	THF
I	0.30	1.30
Br	0.10	0.20
Cl	0.04	n.d.

[a] $PhPdX(PPh_3)_2 + AcO^- \leftrightarrows PhPd(OAc)(PPh_3)_2 + X^-$ K (24).

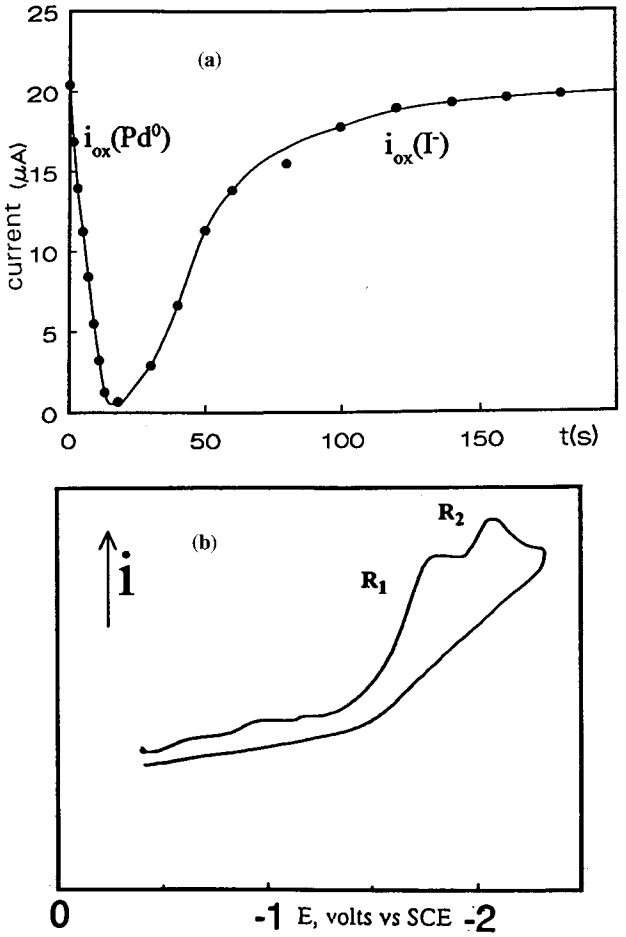

Fig. 13. (a) Oxidative addition of PhI with the palladium(0) complex generated in situ from $Pd(OAc)_2$ (2 mmol dm^{-3}) and PPh_3 (20 mmol dm^{-3}), in DMF (containing n-Bu_4NBF_4, 0.3 mol dm^{-3}) at 25°C. Variation of the oxidation plateau current of the palladium(0) complex at +0.4 V, at a rotating gold disk electrode (i.d. 2 mm; $\omega = 105$ $rad.s^{-1}$) in the presence of phenyl iodide (20 mmol dm^{-3}) as a function of time. (b) Cyclic voltammetry of an authentic sample of $PhPd(OAc)(PPh_3)_2$ (2 mmol dm^{-3}) in DMF (containing n-Bu_4NBF_4, 0.3 mol dm^{-3}) at a stationary gold disk electrode (i.d. 0.5 mm) with a scan rate of 0.2 V s^{-1} at 25°C.

via an anionic pentacoordinated phenylpalladium(II) complex whose half-life time has been estimated to 30 s [18].

Scheme 7 is formally identical to Scheme 6 except for the different life times of the anionic pentacoordinated complexes (30 s *vs.* hours). This emphasizes the role of the anions Cl^- and AcO^- brought by the precursor of the palladium(0). Both anions influence the oxidative addition drastically in the sense that: (i) the structure of the palladium(0) complex; (ii) the rate of the oxidative addition; (iii) the half-life time of the anionic pentacoordinated phenylpalladium(II) complexes; and (iv) the structure of the final complex formed in the oxidative addition, differ as a function of the anion and markedly differ from those invoked in the so-called text book mechanisms.

4.3. Equilibrium between neutral and cationic complexes

^{31}P-NMR spectroscopy shows that in DMF, the complex $PhPd(OAc)(PPh_3)_2$ is involved in an equilibrium with the cationic complex (see Section 4.2) (Eq. (23)). This equilibrium can also be investigated by cyclic voltammetry. Indeed a voltammogram of an authentic sample of *trans* $PhPd(OAc)(PPh_3)_2$ exhibits two successive reduction waves in DMF (Fig. 13b) [18]. The less cathodic one, R_1, features the reduction of the cationic complex whereas the second one, R_2, is the reduction peak of the neutral *trans* $PhPd(OAc)(PPh_3)_2$ complex (its current increases at the expense of that of the cationic complex upon addition of acetate ions).

The same behavior is observed for *trans* $PhPdI(PPh_3)_2$ and $PhPdBr(PPh_3)_2$ formed either by oxidative addition of phenyl iodide with $Pd(0)(PPh_3)_4$ or with the palladium(0) complexes generated in situ in mixture of $Pd(dba)_2 + nPPh_3$. Their cyclic voltammogram exhibits, in DMF, two reduction peaks R_1 and R_2, although both afford a single ^{31}P-NMR signal [40].

$$\underset{(R_1,\ 1e)}{PhPd(PPh_3)_2^+} + X^- \leftrightarrows \underset{(R_2,\ 2e)}{PhPdX(PPh_3)_2}$$

$$K_X (X = Br,\ I,\ OAc)$$

$$K_X = \frac{[PhPdX(PPh_3)_2]}{[PhPd(PPh_3)_2^+][X^-]} \quad (25)$$

This occurs because NMR spectroscopy sees the real status of the solution i.e., only the major species $PhPdX(PPh_3)_2$ (X = I, Br) since the dynamic of the equilibrium is too slow for the NMR time scale (MHz). Conversely, in the voltammetric investigation, the reduction of the cationic complex at R_1 displaces the equilibrium (25) to its left-hand side by continuous consumption of the cationic complex within the diffusion layer. The cationic complex can then be observed even when present at very low concentration at equilibrium (dynamic concentration). This shift depends on

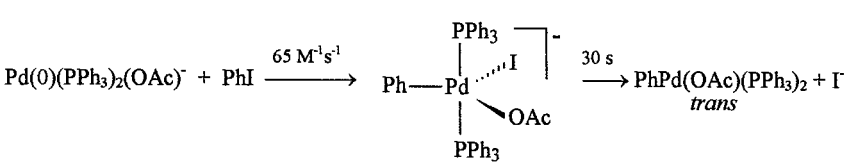

Scheme 7.

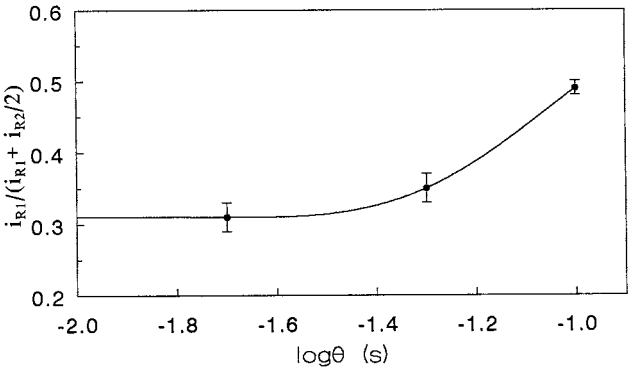

Fig. 14. Variation of the ratio $i_{R_1}/(i_{R_1}+i_{R_2}/2)$ (i, diffusion current determined by chronoamperometry performed on the reduction peaks R_1 and R_2 of $PhPdBr(PPh_3)_2$ (2 mmol dm^{-3}) in DMF containing n-Bu_4NBF_4, 0.3 mol dm^{-3}) as a function of the logarithm of the step duration time θ 20°C.

the time scale of the voltammetric scan. For short times, the equilibrium is frozen. A plot of the relative current i_{R_1} and i_{R_2} of the cationic and neutral complexes *versus* time presents a plateau limit at short times which corresponds to the relative equilibrium concentrations. This plateau value affords the equilibrium constant K_X (Eq. (25)) (Fig. 14 and Table 6) from which one deduces that the affinity of Cl^- for the palladium(II) atom is higher than that of AcO^- [40]. Also from plots such as those in Fig. 14, one can deduce the time scale in which the equilibrium starts to unfreeze. This is given by the departure of the relative current plot from its short time plateau. Fig. 14 shows that for X = Br, the equilibrium becomes labile for $t \geq 50$ ms.

Thus, in DMF, neutral $ArPdX(PPh_3)_2$ (X = I, Br, Cl, OAc) complexes are involved in a moderately fast equilibrium with cationic arylpalladium(II) complexes. The cationic complexes might be more reactive with nucleophiles [41,42] than the neutral complexes and even if present at a small equilibrium concentration might be the real reactive species. Moreover along a catalytic process, the relative concentrations of the cationic and neutral complexes might vary, because controlled by the evolution of the relative concentration of anions and cations which are released in the medium while the catalytic cycles proceed.

Table 6
Equilibrium constant K_X in DMF at 20°C[a]

X	K_X (mol^{-1} dm^3)
Cl	19×10^3
Br	3.6×10^3
I	1.7×10^3
OAc	0.75×10^3

[a] $PhPd(PPh_3)_2^+ + X^- \leftrightarrows PhPdX(PPh_3)_2$ K_X (25).

4.4. Conclusion

Oxidative addition with aryl halides lead to a large variety of arylpalladium(II) complexes: neutral, anionic or cationic complexes [43]. Moreover, these complexes may be linked by dynamic equilibria. The structure of arylpalladium(II) complexes strongly depends on the structure of the effective palladium(0) complex involved in the oxidative addition and are affected by the anions ligated to the palladium(0). We will now examine the influence of the arylpalladium(II) complexes on nucleophilic attacks involved in two important processes: cross-coupling reactions and Heck reactions.

5. Reaction of arylpalladium(II) with nucleophiles

5.1. Mechanism of palladium-catalyzed cross-coupling reactions

$$ArX + Nu^- \xrightarrow{[Pd]} ArNu + X^-$$
$$Pd = Pd(0)(PPh_3)_4,\ \{PdCl_2(PPh_3)_2 + Nu^- \text{ or } H^-\} \quad (26)$$

Discovered in 1976 with Grignard and organolithium reagents as nucleophiles by Fauvarque et al. [5a], this reaction efficient for the formation of C–C bonds, was successively extended to organozinc, aluminum (Negishi et al. [1a,44]), stannyl (Stille et al. [45]) and borane (Suzuki et al. [46]) derivatives [47]. The postulated mechanism is given in Scheme 8a.

For low reactive aryl bromides, the rate determining step is probably the oxidative addition (Eq. a) [5] whereas for more reactive aryl iodides, transmetallation (nucleophilic attack on the *trans* $ArPdXL_2$ complexes, Eq. b) is considered as the rate determining step [48]. Reductive elimination from *trans* $ArPdNuL_2$ complexes is also evoked as the rate determining step (Eqs c + d) [6,49]. However, all these mechanistic studies have been made on different isolated systems, each featuring one step of the postulated cycle and not in the context of a whole catalytic cycle. In particular, it is worth to recall that it has been observed that nucleophilic attacks of Grignard or zinc enolates on *trans* $ArPdI(PPh_3)_2$ complexes (Eq. b in Scheme 8a) provide the coupling product yet with a rate smaller than the rate of the catalytic reaction [5], suggesting that the *trans* $ArPdX(PPh_3)_2$ complex is not involved in the catalytic cycle. A simple way to escape this difficulty consists in admitting that the real intermediate was a *cis* $ArPdX(PPh_3)_2$ complex which must be first formed in the oxidative addition [50]. Nucleophilic attack on the *cis* complex would then afford a *cis* $ArPdNuL_2$ complex and the cross-coupling product after a reductive elimination (Eq. d in Scheme 8a) and so the endergonic *trans*–*cis* isomerization (Eq. c) would be by-passed.

However, in Sections 3 and 4, we have seen that the palladium(0) complex, generated by reduction of $PdCl_2(PPh_3)_2$, is an anionic complex $Pd(0)(PPh_3)_2Cl^-$ so that the oxidative addition affords an anionic pentacoordinated arylpalladium(II) complex, $ArPdXCl(PPh_3)_2^-$ which provides, over long time periods, the expected *trans* $ArPdX(PPh_3)_2$ [38]. In fact, this slow reaction proceeds through a very fast but extremely up-hill pre-equilibrium in which the anionic pentacoordinated arylpalladium(II) complex releases the chloride ion (Scheme 6). Since in our conditions, Cl^- was the best nucleophile and in the same time the best leaving group, this fast up-hill equilibrium represents in fact a degenerate nucleophilic substitution proceeding through a S_N1 mechanism (Eq. 27):

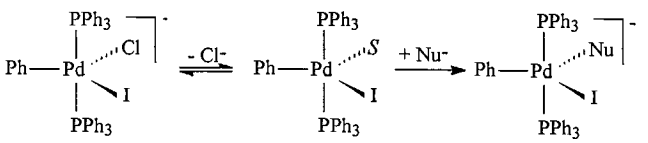

(27)

Therefore, the mechanism that we characterize in this degenerate version is certainly a good representation for the actual nucleophilic substitution at the arylpalladium(II) complex generated by oxidative addition to anionic palladium(0) complex (Eq. 27). This enables to propose a new catalytic cycle (Scheme 8b). The *trans* $ArPdX(PPh_3)_2$ complex may be formed but only at long time and as a terminal route. Consequently the nucleophile attacks the intermediate pentacoordinated neutral arylpalladium(II) complex (Eq. b′ in Scheme 8b), giving rise to an anionic pentacoordinated complex $ArPdXNuL_2^-$ in which the Ar and Nu groups are adjacent and in a favorable position allowing therefore a fast reductive elimination (Eq. d′). As a proof for this new mechanism, the anion 2-thiophenyl (electrogenerated from the bielectronic reduction of 2-iodothiophene) was reacted as a nucleophile with either the *trans* $PhPdI(PPh_3)_2$ complex or with the electrogenerated $PhPdICl(PPh_3)_2^-$ complex. For the same reaction time, the yield in the coupling product 2-Th-Ph was 50% with the *trans* neutral complex and 85% with the anionic complex, showing that the reactivity of the anionic complex is ca. 2.5 times larger than that of the usually postulated *trans* $ArPdXL_2$ complex [51].

We can therefore exclude the *trans* $ArPdXL_2$ complex as intermediate for the cross-coupling reaction when this reaction is catalyzed by $PdCl_2(PPh_3)_2$. However, when the oxidative addition is performed from the palladium(0) complex generated by reduction of $PdCl_2(PPh_3)_2$ in the presence of extra phosphine, the *trans* less reactive $ArPdXL_2$ is formed in a fast phosphine-catalyzed reaction from the pentacoordinated anionic species. This excludes a priori reactions of the nucleophile with the intermediate pentacoordinated arylpalladium(II) complex as proposed in the new mechanism in Scheme 8b. However this observation is made on one isolated step and the competition between PPh_3 and Cl^- to stabilize $Pd(0)(PPh_3)_2$ is in favor of PPh_3 due to the low chloride concentration. However, when the catalytic reaction proceeds, the concentration of halides, released from the aryl halides ArX, increases and the new mechanism which proceeds via anionic

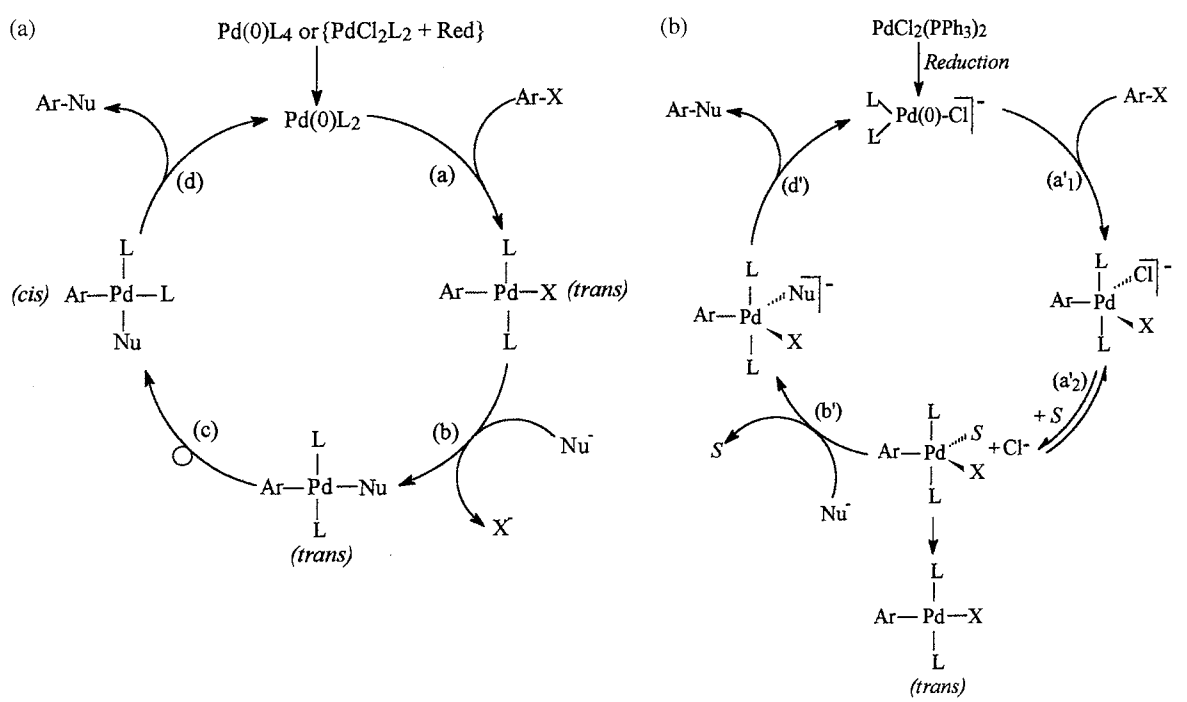

Scheme 8. (a) Postulated mechanism. (b) New catalytic cycle.

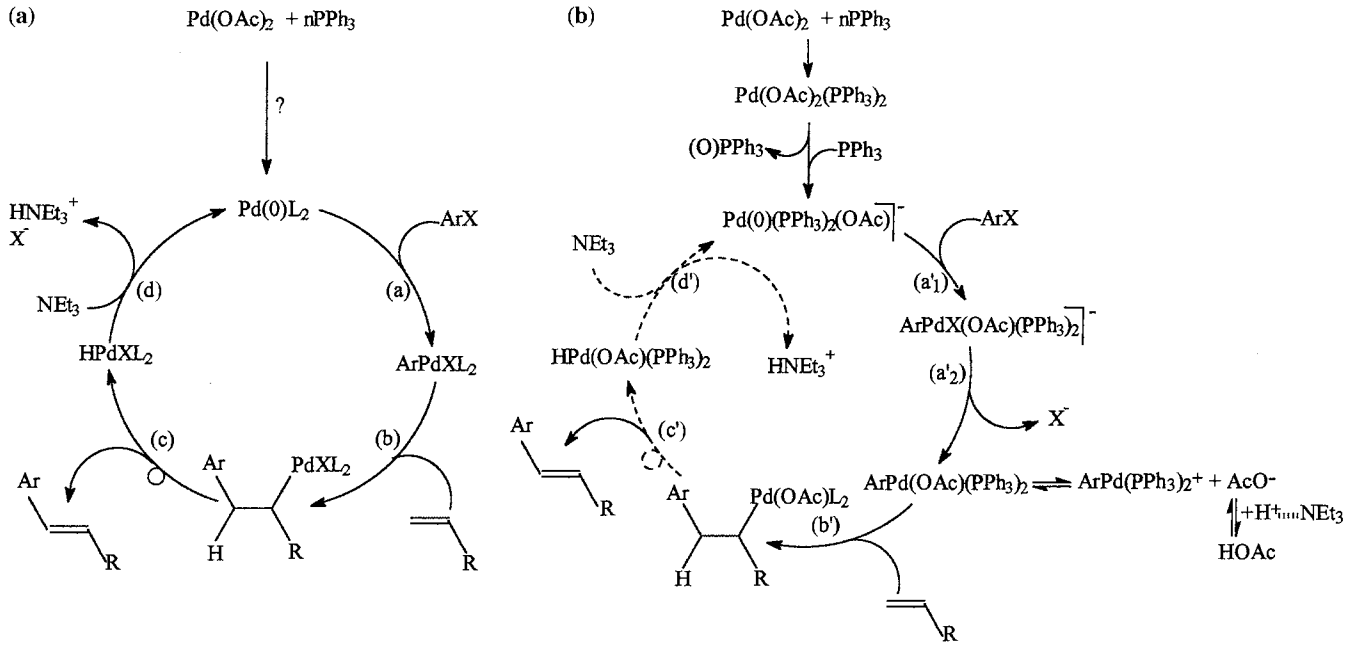

Scheme 9. (a) Postulated mechanism. (b) New catalytic cycle.

species should be more and more efficient. This will also occur in reactions catalyzed by $Pd(PPh_3)_4$. Starting from the reduction of $PdCl_2(PPh_3)_2$, we have also observed that in the absence of any nucleophile, the formation of the *trans* $PhPdI(PPh_3)_2$ is accelerated by cations [38]. This arises from the shift of the equilibrium a'_2 (Scheme 8b) to its left-hand side. If the nucleophile is strong enough to compete with the formation of the *trans* complex, Scheme 8b will be operating. It is therefore seen that the mechanistic features are extremely intricate and that the mechanism may actually change while the catalytic cycle proceeds because the reaction conditions change. Similarly, changes in the reaction medium (e.g. solvent) may also affects the delicate interplay between the two limit cycles in Scheme 8, because ions pairing effects will control the availability of halide ions (released by the aryl halides) and cations (accompanying the nucleophiles). Discussion of the efficiency of a palladium-catalyzed cross-coupling reactions as a function of the nucleophiles shall include all these arguments.

5.2. Mechanism of the Heck reaction

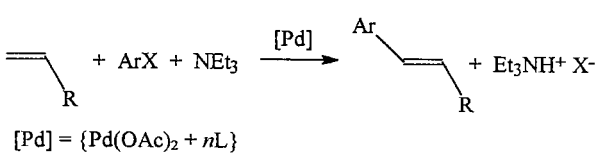

(28)

This reaction, discovered in 1968 by Heck et al. [52], has been considerably extended and developed during the last 15 years [1f]. Enantioselective reactions can now be performed in the presence of chiral ligands [1f, 7]. This reaction requires a base and is usually performed in DMF. Yet it is compatible with aqueous media in the presence of hydrosoluble ligands [53]. The postulated mechanism is represented in Scheme 9a.

Among all the catalytic systems empirically tested for the Heck reaction, mixtures of $Pd(OAc)_2$ and phosphines ligands prove to be efficient. In Section 3.2, we have established that the phosphine reduces the palladium(II) to palladium(0) [16,18,19]. This very first step of the reaction is now proposed in a new catalytic cycle (Scheme 9b). Moreover we have shown that the palladium(0) generated in situ is an anionic species, $Pd(0)(PPh_3)_2(OAc)^-$ which undergoes an oxidative addition with aryl halides through the involvement of a short lived anionic pentacoordinated arylpalladium(II) complex. This anionic complex does not afford the $ArPdX(PPh_3)_2$ complex as expected and postulated in Scheme 9a (Eq. A) but instead gives the *trans* $ArPd(OAc)(PPh_3)_2$ complex (Eqs a'_1 and a'_2 in Scheme 9b). A third arylpalladium(II) complex also exists in solution since $ArPd(OAc)(PPh_3)_2$ is involved in an equilibrium with the cationic $ArPd(PPh_3)_2^+$ complex. Thus, two new stable arylpalladium(II) complexes are expectable candidates for the reaction with alkenes.

Trans $PhPd(OAc)(PPh_3)_2$ formed in the oxidative addition of PhI (one equivalent) with the palladium(0) complex generated in situ in the mixture of $Pd(OAc)_2$ and $4PPh_3$, reacts with styrene (100 equivalents) at room temperature, in DMF, to afford *trans* stilbene as in Heck reaction [18]. The reaction affords better yields in the presence of NEt_3 (compare entries 1–3 of Table

Table 7
Reaction of styrene[a] with phenylpalladium(II) complexes in DMF at 25°C

No.	$PhPdX(PPh_3)_2$	NEt_3 (equivalent/Pd)	t (h)	(*E*)-stilbene (%)[b]
1	$PhPd(OAc)(PPh_3)_2$[c]	0	20	35
2	$PhPd(OAc)(PPh_3)_2$[c]	1[d]	17	70; 70
3	$PhPd(OAc)(PPh_3)_2$[c]	3[d]	19	75; 66
4	$PhPdI(PPh_3)_2$[e]	0	24	0
5	$PhPdI(PPh_3)_2$[e] + $2AcO^-$	0	22	57
6	$PhPdI(PPh_3)_2$[e] + $2AcO^-$	1	48	72
7	$PhPd(PPh_3)_2^+$, BF_4^-[f]	0	25	27
8	$PhPd(PPh_3)_2^+$, BF_4^-[f]	1	18	22

[a] Styrene/$PhPdX(PPh_3)_2$ = 100/1. 0.024 mmol of phenylpalladium(II) complex in 12 ml of DMF.
[b] Yields are relative to the initial phenylpalladium(II) complex.
[c] Reactions performed on $PhPd(OAc)(PPh_3)_2$ resulting from the oxidative addition of PhI (one equivalent) with the palladium(0) complex generated in situ from $Pd(OAc)_2 + 4PPh_3$.
[d] NEt_3 is introduced at the beginning of the reaction together with the mixture $Pd(OAc)_2 + 4PPh_3$.
[e] Reactions performed on an authentic sample of $PhPdI(PPh_3)_2$ in the absence or presence of n-Bu_4NOAc.
[f] Reactions performed on an authentic sample of [$PhPd(PPh_3)_2^+$, BF_4^-].

7). *Trans* $PhPdI(PPh_3)_2$ complex does not react with styrene [54]. However, addition of acetate ions makes the reaction proceed noticeably without any influence of the base (entries 4–6 in Table 7). This is easily rationalized since in Section 4.2, we have seen that acetate ions substitute the iodide of *trans* $PhPdI(PPh_3)_2$ complex to afford *trans* $PhPd(OAc)(PPh_3)_2$ (Eq. 24) which then reacts with styrene. Note that the reactivity of the intermediate anionic pentacoordinated species $PhPdI(OAc)(PPh_3)_2^-$ although not suspected (negatively charged 18-electron complex) has been nevertheless tested by introduction of the styrene just before that of PhI, so that this short-lived intermediate is in contact with the styrene as soon as it is generated. No acceleration of the formation of stilbene has been observed.

Since $PhPd(OAc)(PPh_3)_2$ is in equilibrium with the cationic complex $PhPd(PPh_3)_2^+$, this later could be involved in the reaction with styrene. In fact, [$PhPd(PPh_3)_2^+$, BF_4^-] actually reacts with styrene, however the reaction is slower than that of $PhPd(OAc)(PPh_3)_2$. The reaction affords lower yields in stilbene and is not influenced by the presence of NEt_3 (compare entries 1 and 7, 2 and 8 in Table 7). The reaction of the solvated cationic *trans* $PdPd(PPh_3)_2S^+$ complex with styrene is probably slower because a *trans* complex is formed (Eq. 29), a configuration which in not in favor of a *syn* insertion of the olefin into the Ph–Pd bond which then requires an endergonic *trans*–*cis* isomerization.

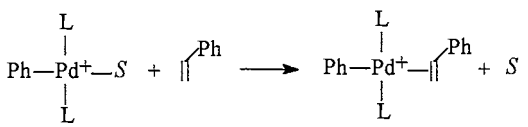

trans (29)

The above series of experiments thus definitively establish that $PhPd(OAc)(PPh_3)_2$ is a key reactive intermediate of the Heck reaction. It reacts with the alkene in the rate determining step of the catalytic cycle (Eq. b′ in Scheme 9b).

The reaction of $PhPd(OAc)(PPh_3)_2$ with styrene is inhibited by excess phosphines which demonstrates that a free coordination site is required to allow coordination of the olefin. In this context, two explanations may be invoked to explain the higher reactivity of $PhPd(OAc)(PPh_3)_2$ compared to that of $PhPdI(PPh_3)_2$. The acetate ligand may assist the liberation of a coordination site (Eq. 30):

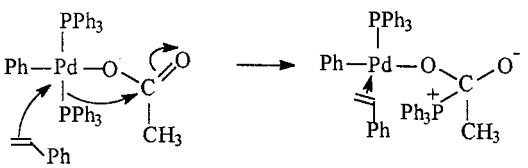

(30)

or protect the free coordination site left by the phosphine owing to its potential bidentate character (Eq. 31):

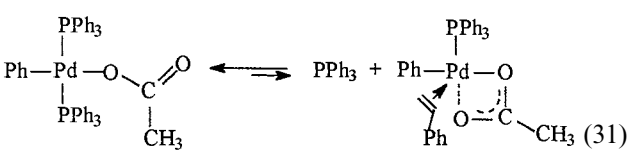

(31)

In both cases, the coordinated olefin would be in a *cis* position compared to the phenyl ligand, a factor which favors the subsequent insertion of the olefin into the Ph–Pd bond.

5.3. Role of the base in the Heck reaction

We do not observe any effect of the base (NEt_3) on the yield in stilbene when starting from PhPd-

$(OAc)(PPh_3)_2$ generated by reaction of AcO^- with $PhPdI(PPh_3)_2$ or from isolated $[PhPd(PPh_3)_2^+, BF_4^-]$, i.e. under conditions in which no protons are present. The only beneficial effect of the base is observed with $PhPd(OAc)(PPh_3)_2$ when it is generated in situ from mixtures of $Pd(OAc)_2$ and phosphine, i.e. together with protons (Section 3.2, Eq. (9)). As shown in Scheme 9b, the equilibrium between the neutral $PhPd(OAc)(PPh_3)_2$ and cationic $PdPd(PPh_3)_2^+$ complex can be displaced by protons through interaction with the acetate ligand also involved in the equilibrium. This interaction shifts the equilibrium in favor of the cationic less reactive complex. Addition of a base to neutralize the protons shifts this equilibrium towards the more reactive species $PhPd(OAc)(PPh_3)_2$. Consequently, the yield in stilbene improves. This phenomenon has also been observed in ^{31}P-NMR spectroscopy. Indeed, when $PhPd(OAc)(PPh_3)_2$ is generated in situ from $Pd(OAc)_2$, the magnitude of the signal of the cationic $PdPd(PPh_3)_2^+$ complex decreases relative to that of the neutral $PhPd(OAc)(PPh_3)_2$, in the presence of NEt_3.

Usually the role of the base is ascribed to the recycling of the palladium(0) catalyst from a palladium(II) hydride complex formed after the β-elimination step (Eq. d in Scheme 9a). However, we observe that the base may also play other more subtle roles. To illustrate the effects of the base, we considered only one cycle of the Heck reaction (only one equivalent of PhI *vs.* Pd) so that the role of the base on the regeneration of the palladium catalyst is irrelevant.

- NEt_3 accelerates the rate determining step of the catalytic cycle, i.e. the very reaction of the olefin with $PhPd(OAc)(PPh_3)_2$ (Eq. b′ in Scheme 9b), by maintaining a high concentration of $PhPd(OAc)(PPh_3)_2$ relative to that of the less reactive cationic intermediate, through neutralization of the protons (note that protons are formed all along the catalytic cycle through reactions c′ and d′ in Scheme 9b).
- NEt_3 slows down a fast step: the oxidative addition with aryl halides (Eq. a_1') as seen above (Section 3.2). Indeed, the base stabilizes the anionic complex $Pd(0)(PPh_3)_2(OAc)^-$ against decomposition by protons and consequently the oxidative addition is slower.

This double effect of the base which tends to accelerate slow reactions and decelerate fast reactions is in favor of a more efficient catalytic cycle by bringing every step to react with comparable rates (see Section 1).

Taking all these facts into consideration (role of acetate ions, role of the base) led us to propose a new mechanism for the Heck reaction (Scheme 9b) in which the crucial role of the acetate ion is fully understood. Indeed, the acetate ion is ligated to every palladium(0) or palladium(II) complexes of the catalytic cycle and mainly on the complex $ArPd(OAc)(PPh_3)_2$ involved in the rate determining step in which this complex reacts with the olefin. This supports the empirical observation that catalytic systems consisting of mixtures of $Pd(OAc)_2$ and phosphines are very efficient catalysts for the Heck reaction from aryl halides. Obviously, some $Pd(0)L_4$ complexes prove to be also catalysts, however under these conditions, acetate ions are often added as a base instead of NEt_3 [1f].

6. Conclusions

Electrochemical techniques associated to other spectroscopic techniques (UV, NMR) provide exceptionally useful information for the elucidation of mechanisms of palladium-catalyzed reactions. Thus, mechanism of elemental steps has been investigated and understood in the context of real catalytic reactions which leads to the proposal of more adequate catalytic cycles for cross-coupling reactions and Heck reactions. Importantly, these new cycles give support and help to rationalize empirical findings dispersed in literature. The fundamental role of chloride or acetate ions brought by palladium(II) complexes, precursors of palladium(0) complexes, has been established. New reactive anionic species are proposed in which the palladium(0) is ligated by chloride or acetate ions. As a consequence, the reactivity of such anionic palladium(0) complexes in oxidative addition strongly depends on these anions, as well as the structure of the final arylpalladium(II) complexes formed in the oxidative addition. Intermediate anionic pentacoordinated arylpalladium(II) complexes are also involved and their stability depends on the nature of the anion (halide or acetate) borne by the palladium(0) complex. Consequently, nucleophilic attack on arylpalladium(II) complexes also strongly depends of these anions. This explains the apparent paradox that palladium(0) and palladium(II) complexes seem to keep in memory their mode of preparation. Indeed, the anions brought in by the precursor then sit on every complex involved in the catalytic cycle. In this review, we mainly focused on the role of anions. However, it is obvious that the nature and availability of the cations brought in, e.g. by the nucleophile, play also a crucial role by indirectly controlling the availability of the anions by ion-pairing effects, as we establish here for protons in the case of the Heck reaction. It is therefore understood that these palladium-catalyzed reactions are incredibly subtle, then being very sensitive to the exact reaction conditions, which is in fact reflected by the so large variety of methods proposed in the literature.

Acknowledgements

This work has been supported in part by the Centre National de la Recherche Scientifique (CNRS, URA

1679, Processus d'Activation Moléculaire), the Ministère de l'Education Nationale et de la Recherche et de la Technologie and the Ecole Normale Supérieure. We are glad to acknowledge the important and active contributions of our former students: Mohamed Azzabi, Emmanuelle Carré, Alain Fuxa, Fouad Khalil, Mohamed Amine M'Barki, Maria José Medeiros, Gilbert Meyer, Loïc Mottier, and Alejandra Suarez whose efforts were crucial in developing this work.

References

[1] For reviews and books on palladium-catalyzed reactions, see: (a) E.I. Negishi, Acc. Chem. Res. 15 (1982) 340. (b) Heck, R.F., Org. React. 27 (1982) 345. (c) R.F. Heck, Palladium Reagents in Organic Synthesis, Academic Press, London, 1985. (d) J.K. Stille, Angw. Chem. Int. Ed. Engl. 25 (1986) 508. (e) K. Ritter, Synthesis (1993) 735. (f) A. de Meijere, F.E. Meyer, Angew. Chem. Int. Ed. Engl. 33 (1994) 2379. (g) W. Cabri, I. Candiani, Acc. Chem. Res. 28 (1995) 2. (h) J. Tsuji, Palladium Reagents and Catalysts: Innovations in Organic Chemistry, Wiley, Chichester, 1995. (i) N. Miyaura, A. Suzuki, Chem. Rev. 95 (1995) 2457. (j) E.I. Negishi, C. Copéret, S. Ma, S.Y. Liou, F. Liu, Chem. Rev. 96 (1996) 365. (k) B.M. Trost, Acc. Chem. Res. 29 (1996) 355. (l) B.M. Trost, D.L. Van Vranken, Chem. Rev. 96 (1996) 395. (m) J.L. Malleron, J.C. Fiaud, J.Y. Legros, Handbook of palladium-catalyzed organic reactions. Synthetic aspects and catalytic cycles, Academic Press, New York, 1997.

[2] (a) A. Jutand, A. Mosleh, J. Org. Chem. 62 (1997) 261. (b) A. Jutand, S. Négri, Eur. J. Org. Chem. (1998) 1811.

[3] (a) P. Fitton, M.P. Johnson, J.E. Mc Keon, J. Chem. Soc. Chem. Commun. (1968) 6. (b) P. Fitton, E.A. Rick, J. Organomet. Chem. 28 (1971) 287.

[4] A. Jutand, A. Mosleh, Organometallics 14 (1995) 1810.

[5] (a) J.F. Fauvarque, A. Jutand, Bull. Soc. Chim. Fr. (1976) 765. (b) J.F. Fauvarque, A. Jutand, J. Organomet. Chem. 132 (1977) C17. (c) idem 177 (1979) 273.

[6] A. Gillie, J.K. Stille, J. Am. Chem. Soc. 102 (1980) 4933.

[7] F. Ozawa, A. Kubo, Y. Matsumoto, T. Hayashi, Organometallics 12 (1993) 4188.

[8] A.J. Bard, L.R. Faulkner, Electrochemical Methods, Wiley, New York, 1980, pp. 443–449.

[9] C. Amatore, M. Azzabi, P. Calas, A. Jutand, C. Lefrou, Y. Rollin, J. Electroanal. Chem. 288 (1990) 45.

[10] B.E. Mann, A. Musco, J. Chem. Soc. Dalton Trans. (1975) 1673.

[11] (a) J.F. Fauvarque, F. Pflüger, M. Troupel, J. Organomet. Chem. 208 (1981) 419. (b) C. Amatore, F. Pflüger, Organometallics 9 (1990) 2276.

[12] A. Sekiya, N. Ishikawa, J. Organomet. Chem. 118 (1976) 349.

[13] (a) C. Amatore, M. Azzabi, A. Jutand, J. Organomet. Chem. 363 (1989) C41. (b) C. Amatore, M. Azzabi, A. Jutand, J. Am. Chem. Soc. 113 (1991) 8375.

[14] The reactivity of $Pd(0)(PPh_3)_2I^-$ could not be determined due to the close vicinity of the oxidation peaks of I^- and $Pd(0)(PPh_3)_2I^-$ [13b].

[15] E.-I. Neghishi, T. Takahashi, K. Akiyoshi, J. Chem. Soc. Chem. Commun. (1986) 1338.

[16] C. Amatore, A. Jutand, M. M'Barki, Organometallics 11 (1992) 3009.

[17] F. Ozawa, A. Kobo, T. Hayashi, Chem. Lett. (1992) 2177.

[18] C. Amatore, E. Carré, A. Jutand, M. M'Barki, G. Meyer, Organometallics 14 (1995) 5605.

[19] C. Amatore, E. Carré, A. Jutand, M. M'Barki, Organometallics 14 (1995) 1818.

[20] Osawa and Hayashi have observed a beneficial effect of water on the rate of formation of $Pd(0)(BINAP)_2$ from mixture of $Pd(OAc)_2$ and BINAP [17].

[21] C. Amatore, A. Jutand, J.L. Ricard, (1996) unpubl. results.

[22] V.V. Grushin, H. Alper, Organometallics 12 (1993) 1890.

[23] C. Amatore, A. Jutand, M.J. Medeiros, New J. Chem. 20 (1996) 1143.

[24] Fluoride anions also induce in water the reduction of $PdCl_2(PPh_3)_2$ by PPh_3 to palladium(0) complexes. See: M.R. Mason, J.G. Verkade, Organometallics 11 (1992) 2212.

[25] C. Amatore, E. Blart, J.P. Genêt, A. Jutand, S. Lemaire-Audoire, M. Savignac, J. Org. Chem. 60 (1995) 6829.

[26] W.A. Herrmann, C. Brossmer, K. Olefe, C.-P. Reisinger, T. Priermeier, M. Beller, H. Fischer, Agnew. Chem. Int. Ed. Engl. 34 (1995) 1844.

[27] For seminal use of mixtures of $Pd(dba)_2$ with bidentate or monodentate phosphine ligands in catalytic reactions, see: (a) J.C. Fiaud, A. Hibon de Gournay, M. Larchevêque, H.B. Kagan, J. Organomet. Chem. 154 (1978) 175. (b) Y. Inoue, T. Hibi, M. Satake, H. Hashimoto, J. Chem. Soc. Chem. Commun. (1979) 982.

[28] (a) C.E. Russell, L.S. Hegedus, J. Am. Chem. Soc. 105 (1983) 943. (b),F. Henin, J.P. Pete, Tetrahedron Lett. 24 (1983) 4687. (c),D. Ferroud, J.P. Genet, J. Muzart, Tetrahedron Lett. 25 (1984) 4379. (d) W. Oppolzer, J.M. Gaudin, Helv. Chem. Acta 70 (1987) 1477. (e) S.I. Murahashi, Y. Taniguchi, Y. Imada, Y. Tanigawa, J. Org. Chem. 54 (1989) 3292.

[29] C. Amatore, A. Jutand, F. Khalil, M.A. M'Barki, L. Mottier, Organometallics 12 (1993) 3168.

[30] W.A. Herrmann, W.R. Thiel, C. Bro(mer, K. Öfele, T. Priermeier, W. Scherer, J. Organomet. Chem. 461 (1993) 51.

[31] The two complexes $SPd(0)(PPh_3)_3$ and $SPd(0)(PPh_3)_2$ are oxidized at the same potential O_1 because they are involved in equilibrium 13 whose forward and backward rates are faster than the voltammetric time scale considered here [29]).

[32] C. Amatore, A. Jutand, G. Meyer, Inorg. Chim. Acta 273 (1998) 76.

[33] C. Amatore, A. Jutand, G. Meyer, H. Atmani, F. Khalil, F. Ouazzani Chahdi, Organometallics 17 (1998) 2958.

[34] The kinetic curves and rate constants are identical whatever the polarization potential (e.g. on O_1 or on O_2) which means that all the palladium(0) complexes are involved in equilibria totally labile during the time scale of the oxidative addition and cannot be kinetically discriminated [29]).

[35] (a) V. Farina, S.R. Baker, D. Begnini, C. Jr. Sapino, Tetrahedron Lett. 29 (1988) 5739. (b) V. Farina, B. Krishna, J. Am. Chem. Soc. 113 (1991) 9585.

[36] C. Amatore, G. Broeker, A. Jutand, F. Khalil, J. Am. Chem. Soc. 119 (1997) 5176.

[37] For a more detailed review see: C. Amatore, A. Jutand, Coord. Chem. Rev. (1999) in press.

[38] C. Amatore, A. Jutand, A. Suarez, J. Am. Chem. Soc. 115 (1993) 9531.

[39] T. Ishiyama, M. Murata, N. Miyaura, J. Org. Chem. 60 (1995) 7508.

[40] C. Amatore, E. Carré, A. Jutand, Acta Chem. Scand. 52 (1998) 100.

[41] (a) As an example $MePd(PMe_3)_2^+$ was found to be 100 times more reactive with CO than the neutral complex $MePdCl(PMe_3)_2$. See: Y. Kayaki, I. Shimizu, A. Yamamoto, Chem. Lett. (1995) 1089. See also (b) Y. Kayaki, F. Kawataka, I. Shimizu, A. Yamamoto, Chem. Lett. (1994) 2171.

[42] See Section 5.2 for Heck reactions where we have shown that the neutral $PdPdI(PPh_3)_2$ does not react with styrene whereas the cationic complex $PdPd(PPh_3)_2^+$, BF_4^- does and affords stilbene [18].

[43] Oxidative addition of aryl triflates with $Pd(PPh_3)_4$ afford cationic $ArPd(PPh_3)_2^+$ complexes. Neutral complexes $ArPdCl(PPh_3)_2$ are formed when the oxidative addition is performed in the presence of chloride ions. See Ref. [4].
[44] E.-I. Neghishi, A.O. King, N. Okukado, J. Org. Chem. 42 (1977) 1821.
[45] D. Milstein, J.K. Stille, J. Am. Chem. Soc. 101 (1979) 4992.
[46] N. Miyaura, K. Yamada, A. Suzuki, Tetrahedron Lett. 20 (1979) 3437.
[47] Creation of C–O ([47]a, b), C–N ([47]c, d) and C–C ([47]e, f) bonds has been achieved from alkoxides, amides and ketone enolates, respectively in the presence of bidentate phosphine ligated palladium. See (a) M. Palucki, J.P. Wolfe, S.L. Buchwald, J. Am. Chem. Soc. 118 (1996) 10333. (b) G. Mann, J.F. Hartwig, J. Am. Chem. Soc. 118 (1996) 13109. (c) F. Paul, J. Patt, J.F. Hartwig, J. Am. Chem. Soc. 116 (1994) 5969. (d) A.S. Guram, R.A. Rennels, S.L. Buchwald, Angew. Chem. Int. Ed. Engl. 35 (1995) 1348. (e) M. Palucki, S.L. Buchwald, J. Am. Chem. Soc. 119 (1997) 11108. (f) B.C. Hamann, J.F. Hartwig, J. Am. Chem. Soc. 119 (1997) 12382.
[48] E.-I. Neghishi, T. Takahashi, S. Baba, D.E. van Horn, N. Okukado, J. Am. Chem. Soc. 109 (1987) 2393.
[49] (a) M. Loar, J.K. Stille, J. Am. Chem. Soc. 103 (1981) 4174. (b) A. Moravsky, J.K. Stille, J. Am. Chem. Soc. 103 (1981) 4182. (c) F. Osawa, T. Ito, Y. Nakamura, Y.Yamamoto, Bull. Soc. Soc. Jpn. 54 (1981) 5868. (d),K. Tatsumi, Y. Nakamura, S. Komiya, Y. Yamamoto, J. Am. Chem. Soc. 106 (1984) 8181.
[50] (a) A *cis* complex has been isolated in one particular case, see H. Urata, M. Tanaka, T. Fuchikami, Chem. Lett. (1987) 751. (b) Most often the *cis* complex is not detected due to its short life time but nevertheless should be produced when the oxidative addition is performed in the absence of halides.
[51] C. Amatore, A. Fuxa, A. Jutand, (1996) unpubl. results.
[52] R.F. Heck, J. Am. Chem. Soc. 90 (1968) 5518.
[53] (a) A.L. Casalnuovo. J.C. Calabresse, J. Am. Chem. Soc. 112 (1990) 4324. (b) J.P. Genêt, E. Blart, M. Savignac, Synlett (1992) 715.
[54] Some $ArPdX(PPh_3)_2$ complexes react with styrene but under more drastic conditions than ours, at least at 80°C. See (a) H.A. Dieck, R.F. Heck, J. Am. Chem. Soc. 96 (1974) 1133. (b) C.M. Andersson, A. Hallberg, G. Jr. Doyle Daves, J. Org. Chem. 52 (1987) 3529.